

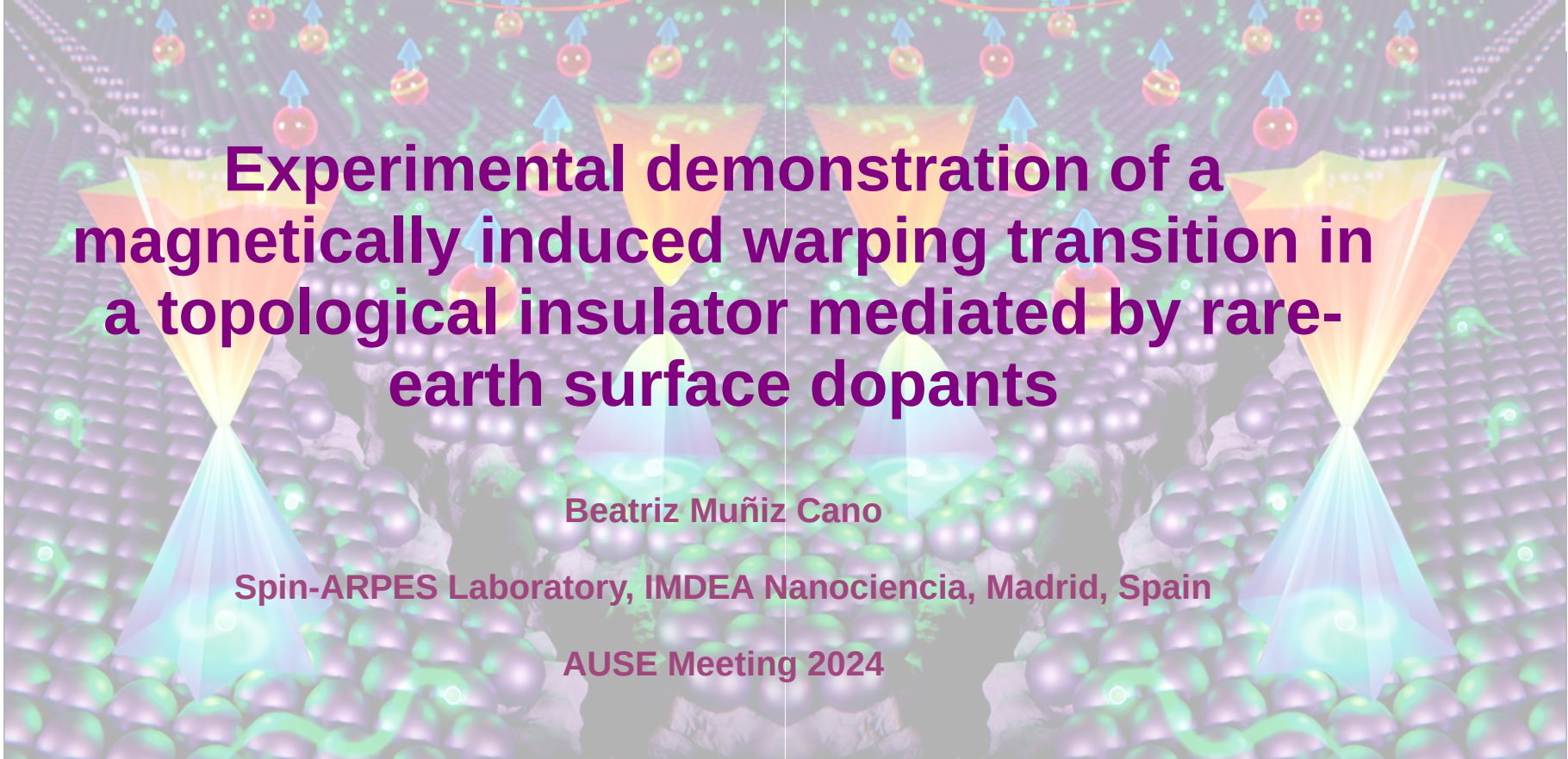


Experimental demonstration of a magnetically induced warping transition in a topological insulator mediated by rare-earth surface dopants

Beatriz Muñiz Cano

Spin-ARPES Laboratory, IMDEA Nanociencia, Madrid, Spain

AUSE Meeting 2024



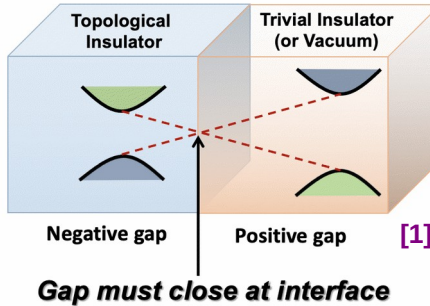


Introduction: topological insulators (TIs)





Introduction: topological insulators (TIs)

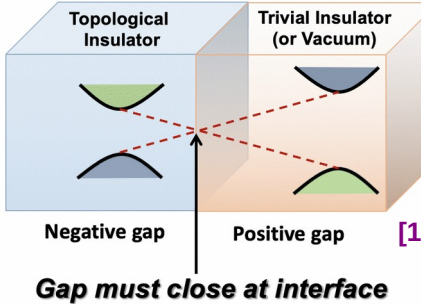


- Topological insulators (TIs) → bulk insulators + **conducting linearly dispersing Dirac edge (surface) states**

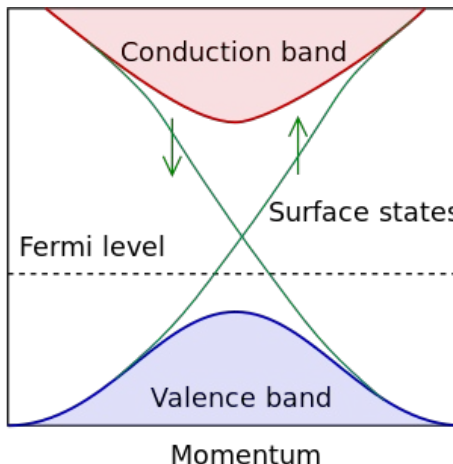
[1] Ruch, T. (2020, November 14). Can you turn a baseball into a donut? An introduction to topological materials [Blog post]. Indiana University Bloomington. <https://blogs.iu.edu/sciu/2020/11/14/can-you-turn-a-baseball-into-a-donut/>.



Introduction: topological insulators (TIs)



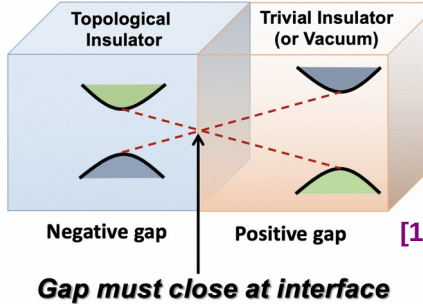
- Topological insulators (TIs) → bulk insulators + conducting linearly dispersing Dirac edge (surface) states
- **Surface states (SS)** are **topologically protected by time-reversal symmetry (TRS)** → topological SS (TSS)



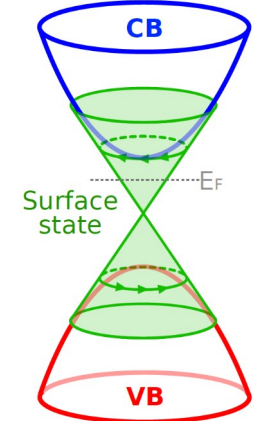
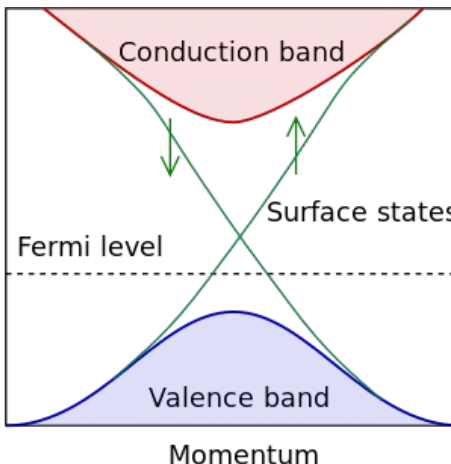
[1] Ruch, T. (2020, November 14). Can you turn a baseball into a donut? An introduction to topological materials [Blog post]. Indiana University Bloomington. <https://blogs.iu.edu/sciu/2020/11/14/can-you-turn-a-baseball-into-a-donut/>.



Introduction: topological insulators (TIs)



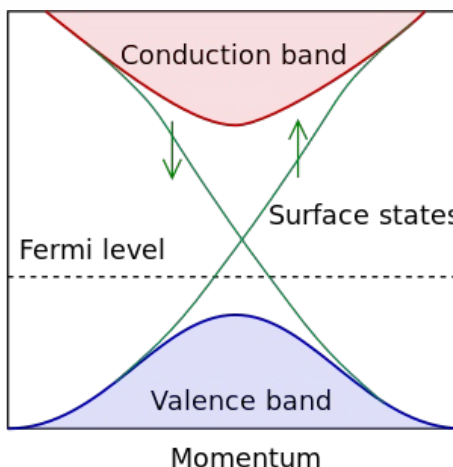
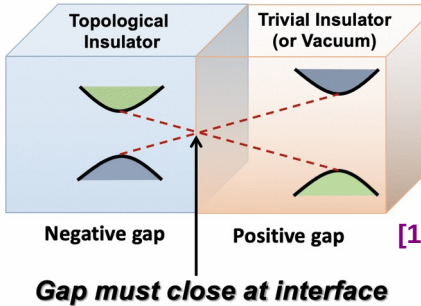
- Topological insulators (TIs) → bulk insulators + conducting linearly dispersing Dirac edge (surface) states
- Surface states (SS) are topologically protected by time-reversal symmetry (TRS) → topological SS (TSS)
- **Large spin-orbit coupling (SOC)**



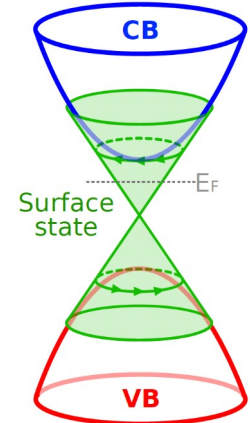
[1] Ruch, T. (2020, November 14). Can you turn a baseball into a donut? An introduction to topological materials [Blog post]. Indiana University Bloomington. <https://blogs.iu.edu/sciu/2020/11/14/can-you-turn-a-baseball-into-a-donut/>. [2] Liu, J.; Hesjedal, T. *Adv. Mat.* **2021**, 2102427.



Introduction: topological insulators (TIs)



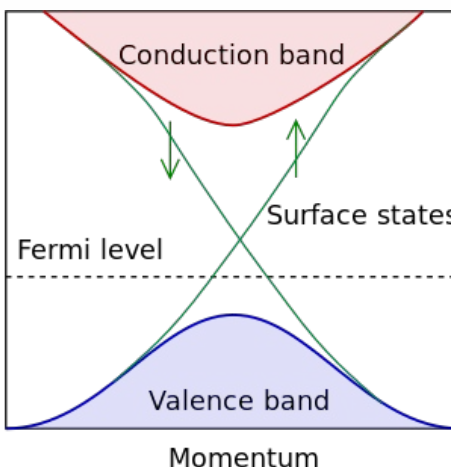
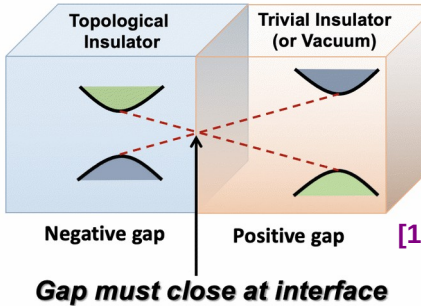
- Topological insulators (TIs) → bulk insulators + conducting linearly dispersing Dirac edge (surface) states
- Surface states (SS) are topologically protected by time-reversal symmetry (TRS) → topological SS (TSS)
- Large spin-orbit coupling (SOC)
- **Topologic robustness + exotic properties → spintronics, quantum computing**



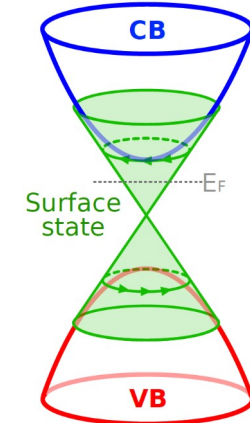
[1] Ruch, T. (2020, November 14). Can you turn a baseball into a donut? An introduction to topological materials [Blog post]. Indiana University Bloomington. <https://blogs.iu.edu/sciu/2020/11/14/can-you-turn-a-baseball-into-a-donut/>.



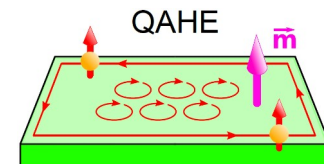
Introduction: topological insulators (TIs)



- Topological insulators (TIs) → bulk insulators + conducting linearly dispersing Dirac edge (surface) states
- Surface states (SS) are topologically protected by time-reversal symmetry (TRS) → topological SS (TSS)
- Large spin-orbit coupling (SOC)
- **Topologic robustness + exotic properties → spintronics, quantum computing**



Disipationless spin-polarized currents
(insulating inside y conductive en el edge)



[1] Ruch, T. (2020, November 14). Can you turn a baseball into a donut? An introduction to topological materials [Blog post]. Indiana University Bloomington. <https://blogs.iu.edu/sciu/2020/11/14/can-you-turn-a-baseball-into-a-donut/>.



Introduction: magnetic TIs (MTIs)





Introduction: magnetic TIs (MTIs)

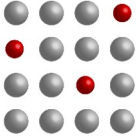
- Impurity magnetic doping





Introduction: magnetic TIs (MTIs)

- **Impurity magnetic doping**

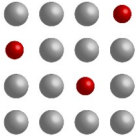


Substitutional or
surface doping [2]

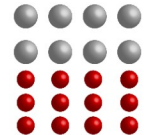


Introduction: magnetic TIs (MTIs)

- **Impurity magnetic doping**



Substitutional or
surface doping [2]



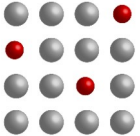
Proximity coupling [3]

[2] Chen, Y. et al. *Science* **2010**, 329, 659–662. [3] Hou, Y et al. *Science adv.* **2019**, 5, eaaw1874.

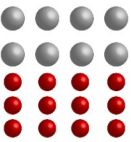


Introduction: magnetic TIs (MTIs)

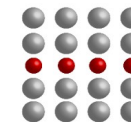
- **Impurity magnetic doping**



Substitutional or
surface doping [2]



Proximity coupling [3]



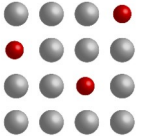
Magnetic extension [4]

[2] Chen, Y. et al. *Science* **2010**, 329, 659–662. [3] Hou, Y et al. *Science adv.* **2019**, 5, eaaw1874. [4] Otrokov, M. M. et al. *JETP Lett.* **2017**, 105, 297–302.

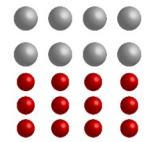


Introduction: magnetic TIs (MTIs)

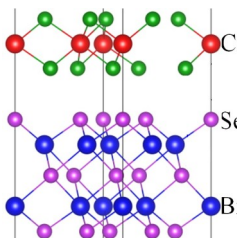
- **Impurity magnetic doping**



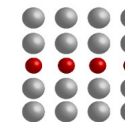
Substitutional or
surface doping [2]



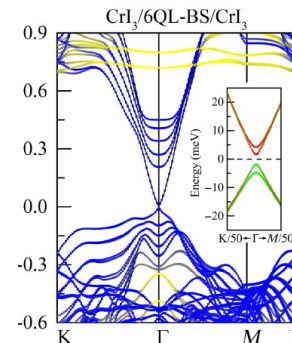
Proximity coupling [3]



[2] Chen, Y. et al. *Science* **2010**, 329, 659–662. [3] Hou, Y et al. *Science adv.* **2019**, 5, eaaw1874. [4] Otrokov, M. M. et al. *JETP Lett.* **2017**, 105, 297–302.



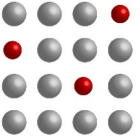
Magnetic extension [4]



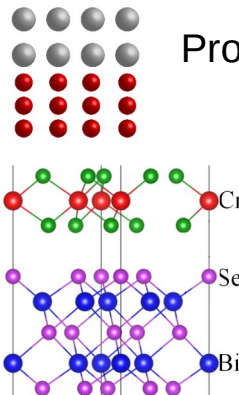


Introduction: magnetic TIs (MTIs)

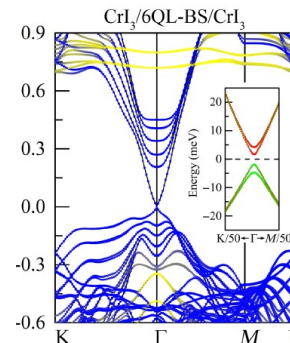
- **Impurity magnetic doping**



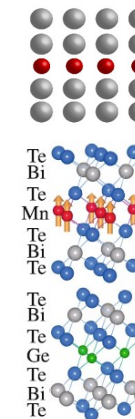
Substitutional or
surface doping [2]



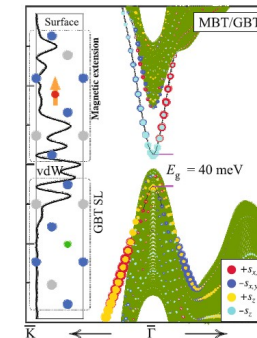
Proximity coupling [3]



[2] Chen, Y. et al. *Science* **2010**, 329, 659–662. [3] Hou, Y. et al. *Science adv.* **2019**, 5, eaaw1874. [4] Otrokov, M. M. et al. *JETP Lett.* **2017**, 105, 297–302.



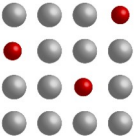
Magnetic extension [4]



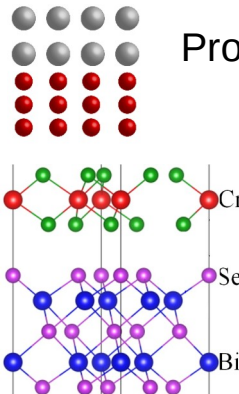


Introduction: magnetic TIs (MTIs)

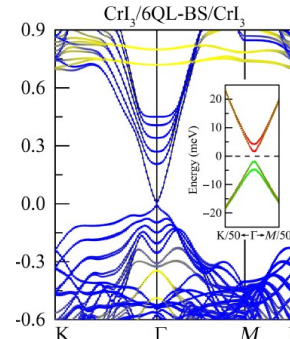
- **Impurity magnetic doping**



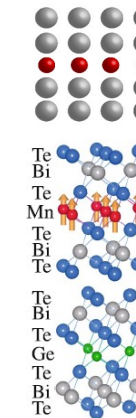
Substitutional or
surface doping [2]



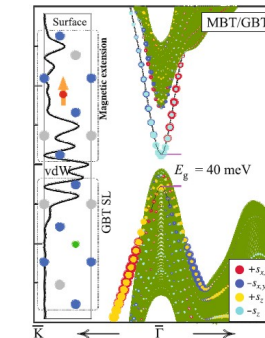
Proximity coupling [3]



[2] Chen, Y. et al. *Science* **2010**, 329, 659–662. [3] Hou, Y. et al. *Science adv.* **2019**, 5, eaaw1874. [4] Otrokov, M. M. et al. *JETP Lett.* **2017**, 105, 297–302. [5] Otrokov, M. M. et al. *Nature* **2019**, 576, 416–422. [6] Rienks, E. D. et al. *Nature* **2019**, 576, 423–428.



Magnetic extension [4]



Prediction and observation of an antiferromagnetic topological insulator [5]

<https://doi.org/10.1038/s41586-019-1840-9>

Received: 20 September 2018

Accepted: 18 September 2019

Published online: 18 December 2019

M. Otrokov^{1,2,3,4}, I. I. Klimovskikh⁴, H. Bentmann⁴, D. Estynin¹, A. Zeugner⁴, Z. S. Alev^{1,6}, S. Gaß⁵, A. U. B. Wolter⁴, A. V. Koroleva⁴, A. M. Shikin⁴, M. Blanco-Rey^{1,2}, M. Hoffmann⁶, I. P. Rusinov^{1,2}, A. Yu. Yuzovskaya^{1,2}, S. V. Eremeev^{1,2,3}, Yu. M. Koroteev^{2,3}, V. M. Kuznetsov^{1,2}, F. Freysoldt¹, J. Sánchez-Barriga^{1,4}, I. R. Amiraslanov⁷, M. B. Babany^{1,6}, N. T. Mamedov⁷, N. A. Abdullaev¹, V. N. Zverev^{1,6}, A. Alfonsov⁸, V. Kataev⁹, B. Büchner^{1,2}, E. F. Schwier¹⁰, S. Kumar¹¹, A. Kimura¹², L. Petaccia¹³, O. Di Santo¹⁰, R. C. Vidal⁹, S. Schatz¹², K. Kübler¹³, M. Ünzelmann¹³, C. H. Min¹⁴, Simon Moser¹¹, F. Reinert¹, A. Ernst^{1,2}, P. M. Echenique^{1,2,3}, A. Isaeva¹⁰ & E. V. Chulkov^{1,2,3,4,6}

Large magnetic gap at the Dirac point in $\text{Bi}_2\text{Te}_3/\text{MnBi}_2\text{Te}_4$ heterostructures [6]

<https://doi.org/10.1038/s41586-019-1826-7>

Received: 10 May 2018

Accepted: 18 October 2019

Published online: 18 December 2019

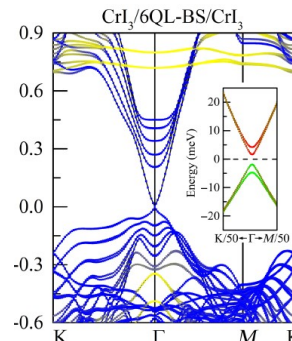
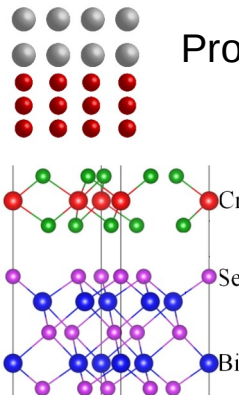
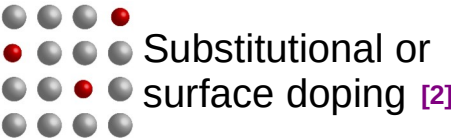
E. D. L. Rienks^{1,2,3,4}, S. Wimmer^{4,5}, J. Sánchez-Barriga^{1,6}, O. Caha^{5,6}, P. S. Mandal⁷, J. Růžička⁸, A. Ney⁹, H. Steiner⁴, V. V. Volobuev^{1,2,3}, H. Grottel⁵, M. Albu¹⁰, G. Kothelchner¹⁰, J. Michaláčka¹⁰, S. A. Khan¹⁰, J. Mihári¹⁰, H. Ebert⁵, G. Bauer⁵, F. Freysoldt¹, A. Varykhov¹, O. Rader¹¹ & G. Springholz⁴



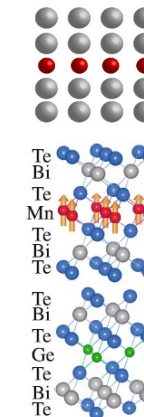


Introduction: magnetic TIs (MTIs)

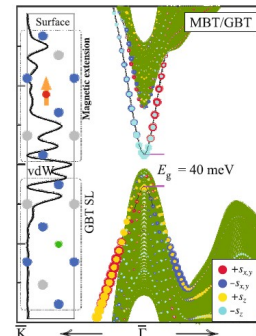
- **Impurity magnetic doping**



[2] Chen, Y. et al. *Science* **2010**, 329, 659–662. [3] Hou, Y. et al. *Science adv.* **2019**, 5, eaaw1874. [4] Otrokov, M. M. et al. *JETP Lett.* **2017**, 105, 297–302. [5] Otrokov, M. M. et al. *Nature* **2019**, 576, 416–422. [6] Rienks, E. D. et al. *Nature* **2019**, 576, 423–428. [7] Garnica, M. et al. *Npj Quant. Mat.* **2022**, 7, 1–9.



Magnetic extension [4]



Prediction and observation of an antiferromagnetic topological insulator [5]

<https://doi.org/10.1038/s41586-019-1840-9>

Received: 20 September 2018

Accepted: 18 September 2019

Published online: 18 December 2019

M. M. Otrokov^{1,2,3,4}, I. I. Klimovskikh⁴, H. Bentmann⁵, D. Estyunin¹, A. Zeugner⁶, Z. S. Aliev^{1,6}, S. Gaß⁷, A. U. B. Wotter⁷, A. V. Koroleva⁸, A. M. Shikin⁴, M. Blanco-Rey^{2,3}, M. Hoffmann⁸, I. P. Rusinov^{1,2}, A. Yu. Yuzovskaya^{1,2}, S. V. Eremeev^{1,2,3}, Yu. M. Koroteev^{2,3}, V. M. Kuznetsov², F. Freysoldt¹, J. Sánchez-Barriga^{1,4}, I. R. Amiraslanov⁹, M. B. Babany¹⁰, N. T. Mamedov¹⁰, N. A. Abdullaev⁷, V. N. Zverev¹⁰, A. Alfonsov¹⁰, B. Büchner¹¹, E. F. Schwier¹¹, S. Kumar¹², A. Kimura¹², L. Petaccia¹², O. Di Santo¹⁰, R. C. Vidal¹², S. Schatz¹², K. Kübler¹², M. Ünzelmann¹², C. H. Min¹², Simon Moser¹², T. R. Peixoto¹², F. Reinert¹², A. Ernst¹², P. M. Echenique^{1,2,3}, A. Isaeva¹⁰ & E. V. Chulkov^{1,2,3,4}

Large magnetic gap at the Dirac point in Bi2Te3/MnBi2Te4 heterostructures [6]

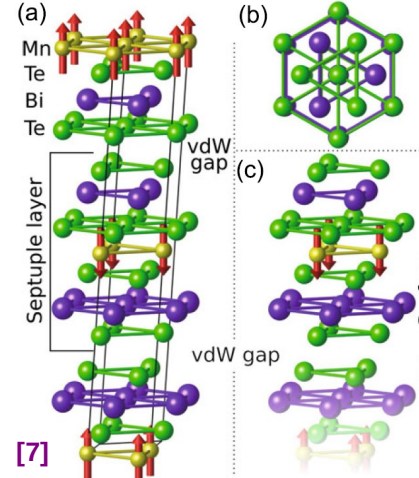
<https://doi.org/10.1038/s41586-019-1826-7>

Received: 10 May 2018

Accepted: 18 October 2019

Published online: 18 December 2019

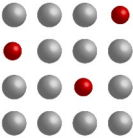
E. D. L. Rienks^{1,2,3,4}, S. Wimmer^{1,4}, J. Sánchez-Barriga^{1,4}, O. Caha^{1,4}, P. S. Mandal^{1,4}, J. Rützicka¹, A. Ney¹, H. Steiner¹, V. V. Volobuev^{1,2,3}, H. Grottel¹, M. Albu^{1,4}, G. Kothelchner^{1,4}, J. Michalek^{1,4}, S. A. Khan¹, J. Mihári¹, H. Ebert^{1,4}, G. Bauer¹, F. Freysoldt^{1,2}, A. Varykhov¹, O. Rader^{1,4} & G. Springholz^{1,4}



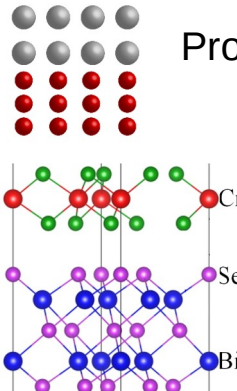


Introduction: magnetic TIs (MTIs)

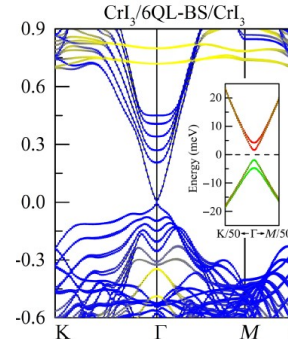
- **Impurity magnetic doping**



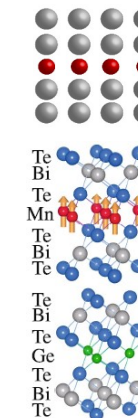
Substitutional or
surface doping [2]



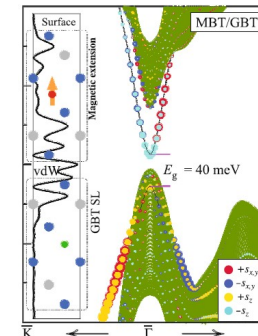
Proximity coupling [3]



[2] Chen, Y. et al. *Science* **2010**, 329, 659–662. [3] Hou, Y. et al. *Science adv.* **2019**, 5, eaaw1874. [4] Otkrov, M. M. et al. *JETP Lett.* **2017**, 105, 297–302. [5] Otkrov, M. M. et al. *Nature* **2019**, 576, 416–422. [6] Rienks, E. D. et al. *Nature* **2019**, 576, 423–428. [7] Garnica, M. et al. *Npj Quant. Mat.* **2022**, 7, 1–9. [8] Grauer, S. et al. *PRB* **2015**, 92, 201304. [9] Pan, L. et al. *Science adv.* **2020**, 6, eaaz3595.



Magnetic extension [4]



Prediction and observation of an antiferromagnetic topological insulator [5]

<https://doi.org/10.1038/s41586-019-1840-9>

Received: 20 September 2018

Accepted: 18 September 2019

Published online: 18 December 2019

M. M. Otkrov^{1,2,3,4}, I. I. Klimovskikh⁴, H. Bentmann⁵, D. Estynin¹, A. Zeugner⁴, Z. S. Aliev^{1,6}, S. Gaß⁷, A. U. B. Wotter⁷, A. V. Koroleva⁸, A. M. Shikin⁴, M. Blanco-Rey^{1,2}, M. Hoffmann⁸, I. P. Rusinov^{1,2}, A. Yu. Yazykovskaya^{1,2}, S. V. Eremeev^{1,2,3}, Yu. M. Koroteev^{2,3}, V. M. Kuznetsov², F. Freysoldt¹, J. Sánchez-Barriga^{1,4}, I. R. Amiraslanov⁹, M. B. Babany¹⁰, N. T. Mamedov¹⁰, A. N. Abdullaev¹⁰, V. N. Zverev¹⁰, A. Alfonsov¹⁰, V. Kataev¹⁰, B. Büchner¹¹, E. F. Schwier¹⁰, S. Kumar¹⁰, A. Kimura¹⁰, L. Petaccia¹⁰, O. Di Santo¹⁰, R. C. Vidal¹⁰, S. Schatz¹⁰, K. Kübler¹⁰, M. Ünzelmann¹⁰, C. H. Min¹⁰, Simon Moser¹⁰, T. R. Peixoto¹⁰, F. Reinert¹⁰, A. Ernst^{1,2}, P. M. Echenique^{1,2,3}, A. Isaeva¹⁰ & E. V. Chulkov^{1,2,3,4}

Large magnetic gap at the Dirac point in Bi₂Te₃/MnBi₂Te₄ heterostructures [6]

<https://doi.org/10.1038/s41586-019-1826-7>

Received: 10 May 2018

Accepted: 18 October 2019

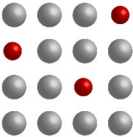
Published online: 18 December 2019

E. D. L. Rienks^{1,2,3,4}, S. Wimmer^{1,4}, J. Sánchez-Barriga^{1,4}, O. Caha^{1,4}, P. S. Mandal^{1,5}, J. Rützka^{1,6}, H. Steiner^{1,6}, V. V. Volobuev^{1,3,7}, H. Grotts¹, M. Albu^{1,6}, G. Kothelchner^{1,6}, J. Michalek^{1,6}, S. A. Khan^{1,6}, J. Mihári^{1,6}, H. Ebert^{1,6}, G. Bauer¹, F. Freysoldt¹, A. Varykhov¹, O. Rader^{1,6} & G. Springholz^{1,6}

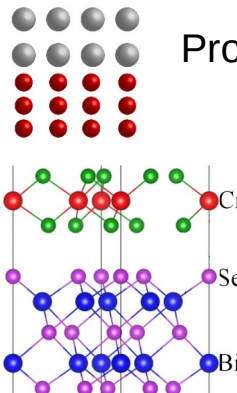


Introduction: magnetic TIs (MTIs)

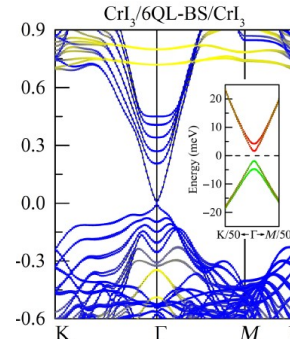
- **Impurity magnetic doping**



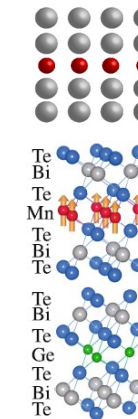
Substitutional or
surface doping [2]



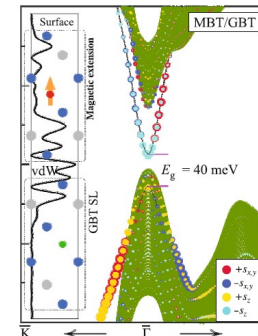
Proximity coupling [3]



[2] Chen, Y. et al. *Science* **2010**, 329, 659–662. [3] Hou, Y. et al. *Science adv.* **2019**, 5, eaaw1874. [4] Otrokov, M. M. et al. *JETP Lett.* **2017**, 105, 297–302. [5] Otrokov, M. M. et al. *Nature* **2019**, 576, 416–422. [6] Rienks, E. D. et al. *Nature* **2019**, 576, 423–428. [7] Garnica, M. et al. *Npj Quant. Mat.* **2022**, 7, 1–9. [8] Grauer, S. et al. *PRB* **2015**, 92, 201304. [9] Pan, L. et al. *Science adv.* **2020**, 6, eaaz3595.



Magnetic extension [4]

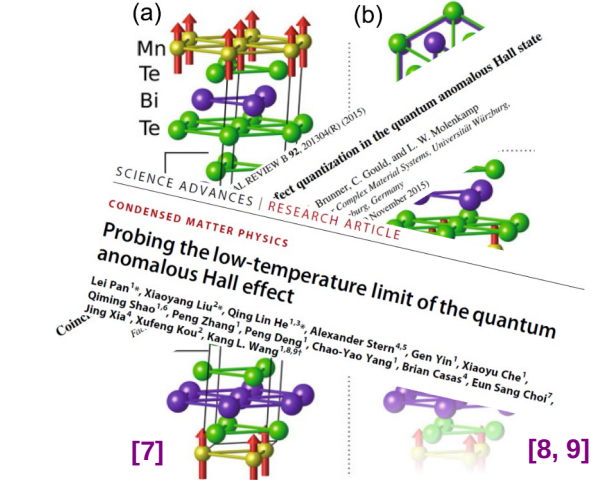


Prediction and observation of an antiferromagnetic topological insulator [5]

<https://doi.org/10.1038/s41586-019-1840-9>
Received: 20 September 2018
Accepted: 18 September 2019
Published online: 18 December 2019

Large magnetic gap at the Dirac point in Bi2Te3/MnBi2Te4 heterostructures [6]

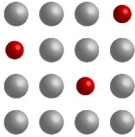
<https://doi.org/10.1038/s41586-019-1826-7>
Received: 10 May 2018
Accepted: 18 October 2019
Published online: 18 December 2019



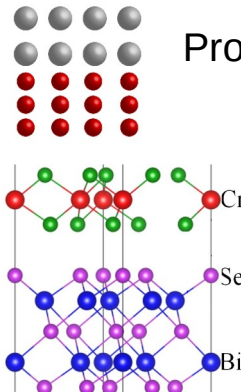


Introduction: magnetic TIs (MTIs)

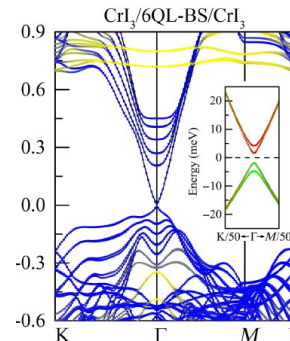
- **Impurity magnetic doping**



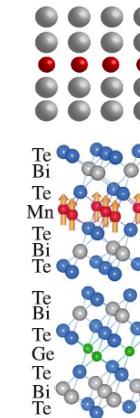
Substitutional or
surface doping [2]



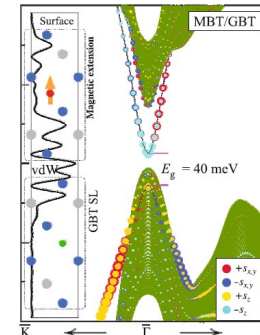
Proximity coupling [3]



[2] Chen, Y. et al. *Science* **2010**, 329, 659–662. [3] Hou, Y. et al. *Science adv.* **2019**, 5, eaaw1874. [4] Otrokov, M. M. et al. *JETP Lett.* **2017**, 105, 297–302. [5] Otrokov, M. M. et al. *Nature* **2019**, 576, 416–422. [6] Rienks, E. D. et al. *Nature* **2019**, 576, 423–428. [7] Garnica, M. et al. *Npj Quant. Mat.* **2022**, 7, 1–9. [8] Grauer, S. et al. *PRB* **2015**, 92, 201304. [9] Pan, L. et al. *Science adv.* **2020**, 6, eaaz3595.



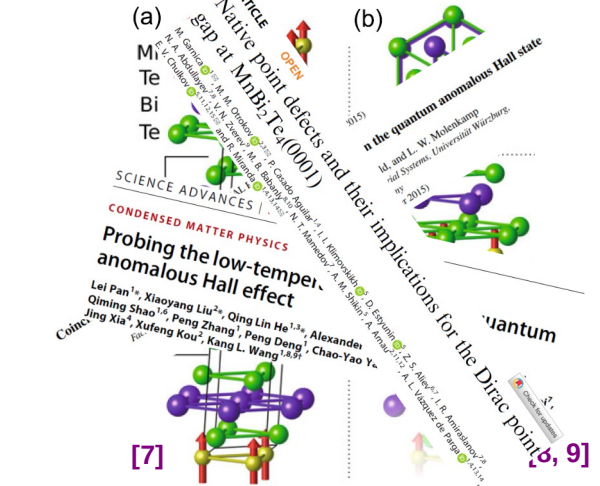
Magnetic extension [4]



Prediction and observation of an antiferromagnetic topological insulator [5]

<https://doi.org/10.1038/s41586-019-1840-9>
Received: 20 September 2018
Accepted: 18 September 2019
Published online: 18 December 2019

<https://doi.org/10.1038/s41586-019-1826-7>
Received: 10 May 2018
Accepted: 18 October 2019
Published online: 18 December 2019



Large magnetic gap at the Dirac point in Bi2Te3/MnBi2Te4 heterostructures [6]

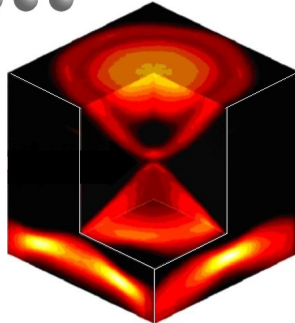
E. D. L. Rienks^{1,2,3*}, S. Wimmer^{4,5}, J. Sánchez-Barriga^{1,6}, O. Caha^{5,6}, P. S. Mandal⁷, J. Rützka⁸, A. Ney⁹, H. Steinert⁹, V. V. Volobuev^{1,10}, H. Grottel¹⁰, M. Albu¹⁰, G. Kothelchner¹⁰, J. Michalek¹⁰, S. A. Khan¹⁰, J. Mihári¹⁰, H. Ebert¹⁰, G. Bauer¹⁰, F. Freysoldt¹⁰, A. Varykhov¹⁰, O. Rader¹⁰ & G. Springholz¹⁰



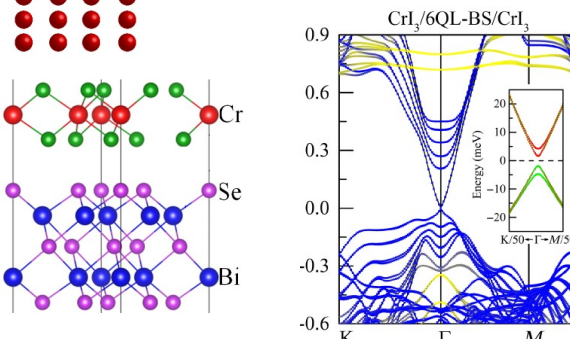
Introduction: magnetic TIs (MTIs)

- **Impurity magnetic doping**

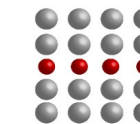
Substitutional or surface doping [2]



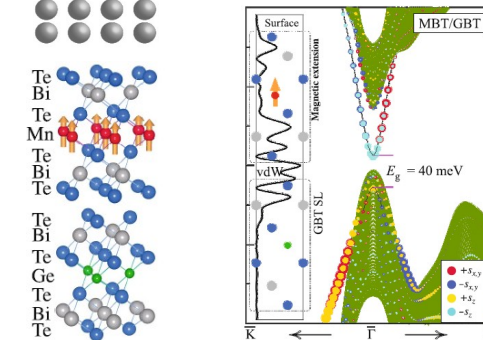
Proximity coupling [3]



[2] Chen, Y. et al. *Science* **2010**, 329, 659–662. [3] Hou, Y. et al. *Science adv.* **2019**, 5, eaaw1874. [4] Otrokov, M. M. et al. *JETP Lett.* **2017**, 105, 297–302. [5] Otrokov, M. M. et al. *Nature* **2019**, 576, 416–422. [6] Rienks, E. D. et al. *Nature* **2019**, 576, 423–428. [7] Garnica, M. et al. *Npj Quant. Mat.* **2022**, 7, 1–9. [8] Grauer, S. et al. *PRB* **2015**, 92, 201304. [9] Pan, L. et al. *Science adv.* **2020**, 6, eaaz3595.



Magnetic extension [4]

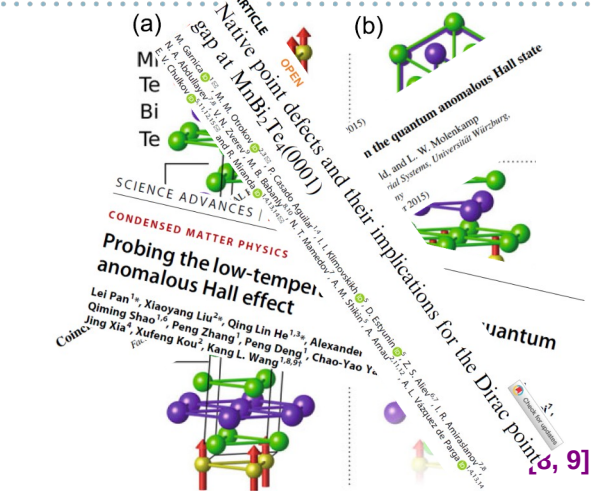


Prediction and observation of an antiferromagnetic topological insulator [5]

<https://doi.org/10.1038/s41586-019-1840-9>
Received: 20 September 2018
Accepted: 18 September 2019
Published online: 18 December 2019

Large magnetic gap at the Dirac point in Bi2Te3/MnBi2Te4 heterostructures [6]

<https://doi.org/10.1038/s41586-019-1826-7>
Received: 10 May 2018
Accepted: 18 October 2019
Published online: 18 December 2019

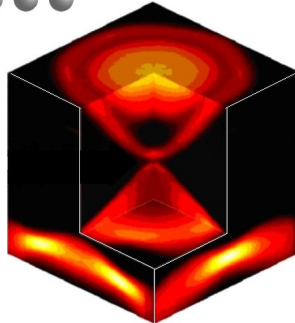




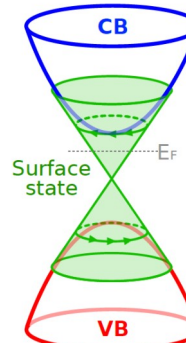
Introduction: magnetic TIs (MTIs)

- **Impurity magnetic doping**

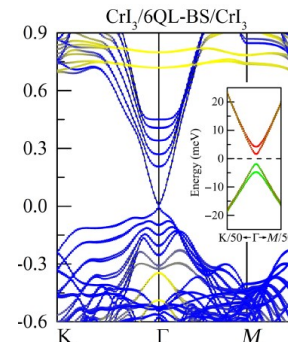
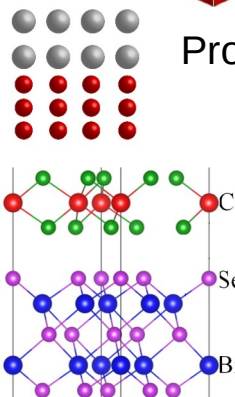
Substitutional or surface doping [2]



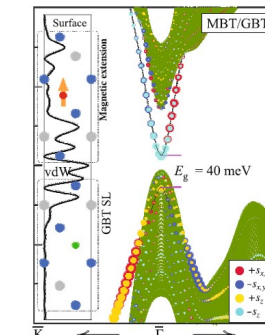
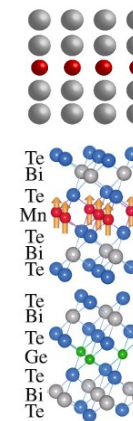
Massless Dirac fermions



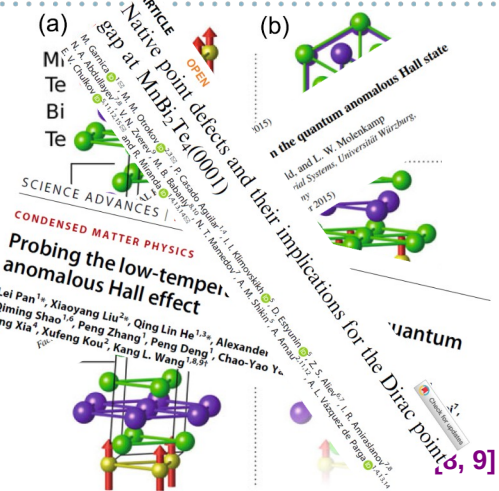
Proximity coupling [3]



Magnetic extension [4]



- [2] Chen, Y. et al. *Science* **2010**, 329, 659–662. [3] Hou, Y. et al. *Science adv.* **2019**, 5, eaaw1874. [4] Otkrov, M. M. et al. *JETP Lett.* **2017**, 105, 297–302. [5] Otkrov, M. M. et al. *Nature* **2019**, 576, 416–422. [6] Rienks, E. D. et al. *Nature* **2019**, 576, 423–428. [7] Garnica, M. et al. *Npj Quant. Mat.* **2022**, 7, 1–9. [8] Grauer, S. et al. *PRB* **2015**, 92, 201304. [9] Pan, L. et al. *Science adv.* **2020**, 6, eaaz3595.



Prediction and observation of an antiferromagnetic topological insulator [5]

<https://doi.org/10.1038/s41586-019-1840-9>
Received: 20 September 2018
Accepted: 18 September 2019
Published online: 18 December 2019

M. M. Otkrov^{1,2,3,4}, I. I. Klimovskikh¹, H. Bentmann¹, D. Estyunin¹, A. Zeugner¹, Z. S. Aliev^{1,6}, S. Gaß¹, A. U. B. Wotter¹, A. V. Koroleva¹, A. M. Shikin¹, M. Blanco-Rey^{2,3}, M. Hoffmann², I. P. Rusinov^{2,3}, A. Yu. Yuzovskaya^{2,3}, S. V. Eremeev^{2,3}, Yu. M. Koroteev^{2,3}, V. M. Kuznetsov^{2,3}, F. Freysoldt¹, J. Sánchez-Barriga^{4,5}, I. Amiraslanov¹, M. B. Babany³, N. T. Mamedov³, N. A. Abdullaev³, V. N. Zverev³, A. Alfonsov³, V. Kataev³, B. Büchner³, E. F. Schwieter³, S. Kumar³, A. Kimura³, L. Petaccia³, O. Di Santo³, R. C. Vidal³, S. Schatz², K. Küller³, M. Ünalzmann³, C. H. Min³, Simon Moser³, T. R. Peixoto³, F. Reinert³, A. Ernst^{1,2,3}, P. M. Echenique^{1,2,3}, A. Isaeva^{3,7} & E. V. Chulkov^{2,3,8}

<https://doi.org/10.1038/s41586-019-1826-7>
Received: 10 May 2018
Accepted: 18 October 2019
Published online: 18 December 2019

E. D. L. Rienks^{1,2,3,4}, S. Wimmer^{1,4}, J. Sánchez-Barriga^{1,4}, O. Caha^{1,4}, P. S. Mandal^{1,5}, J. Rützke¹, A. Ney¹, H. Steiner¹, V. W. Volobuev^{1,4,6}, H. Grottel¹, M. Albu¹, G. Kothelchner¹, J. Michalek¹, S. A. Khan¹, J. Mihári¹, H. Ebert¹, G. Bauer¹, F. Freysoldt¹, A. Varykhov¹, O. Rader^{1,6} & G. Springholz^{1,4}

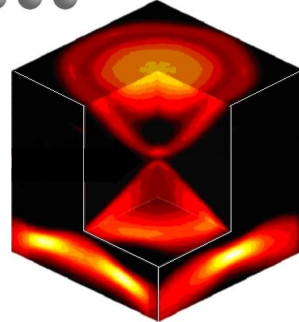
Large magnetic gap at the Dirac point in $\text{Bi}_2\text{Te}_3/\text{MnBi}_2\text{Te}_4$ heterostructures [6]



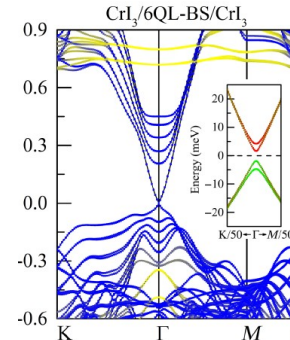
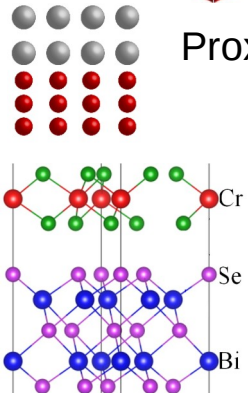
Introduction: magnetic TIs (MTIs)

- **Impurity magnetic doping**

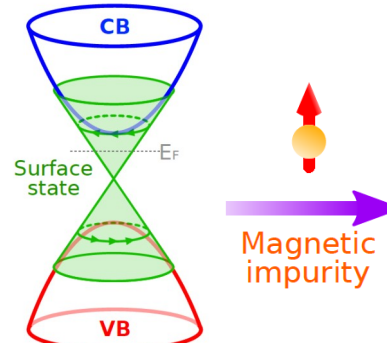
Substitutional or surface doping [2]



- **Proximity coupling [3]**

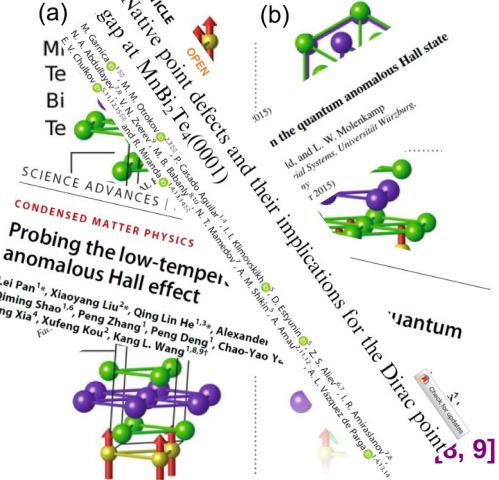
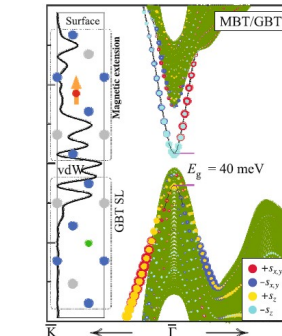
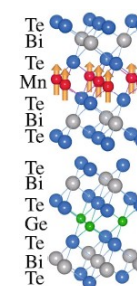
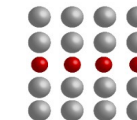


Massless Dirac fermions



Magnetic
impurity

Magnetic extension [4]



Prediction and observation of an antiferromagnetic topological insulator [5]

<https://doi.org/10.1038/s41586-019-1840-9>
Received: 20 September 2018
Accepted: 18 September 2019
Published online: 18 December 2019

M. M. Otrokov^{1,2,3,4}, I. I. Klimovskikh¹, H. Bentmann¹, D. Estyunin¹, A. Zeugner¹, Z. S. Aliev^{1,6}, S. Gaß¹, A. U. B. Wolter¹, A. V. Koroleva¹, A. M. Shikin¹, M. Blanco-Rey^{2,3}, M. Hoffmann², I. P. Rusinov^{2,3}, A. Yu. Yuzovskaya^{2,3}, S. V. Eremeev^{2,3}, Yu. M. Koroteev^{2,3}, V. M. Kuznetsov^{2,3}, F. Freysoldt¹, J. Sánchez-Barriga^{1,4}, I. Amiraslanov¹, M. B. Babany^{1,5}, N. T. Mamedov¹, N. A. Abdullaev¹, V. N. Zverev^{1,6}, A. Alfonsov¹, V. Kataev¹, B. Büchner^{1,7}, F. E. Schwegler¹, S. Kumar¹, A. Kimura¹, L. Petaccia¹, O. Di Santo¹, R. C. Vidal¹, S. Schatz¹, K. Küller¹, M. Ünzelmann¹, C. H. Min¹, Simon Moser¹, T. R. Peixoto¹, F. Reinert¹, A. Ernst^{1,2}, P. M. Echenique^{1,2,3}, A. Isaeva^{1,2} & E. V. Chulkov^{2,3,4,5}

Large magnetic gap at the Dirac point in Bi₂Te₃/MnBi₂Te₄ heterostructures [6]

<https://doi.org/10.1038/s41586-019-1826-7>
Received: 10 May 2018
Accepted: 18 October 2019
Published online: 18 December 2019

D. L. Rienks^{1,2,3,4}, S. Wimmer^{1,4}, J. Sánchez-Barriga^{1,4}, O. Caha^{1,4}, P. S. Mandal^{1,5}, J. Rützke^{1,6}, A. Ney¹, H. Steinleitner¹, V. W. Volobuev^{1,7}, H. Grottel¹, M. Albu^{1,8}, G. Kothelchner^{1,9}, J. Michalek^{1,9}, S. A. Khan^{1,9}, J. Mihári^{1,9}, H. Ebert^{1,9}, G. Bauer¹, F. Freysoldt¹, A. Varykhov^{1,9}, O. Rader^{1,9} & G. Springholz^{1,4}



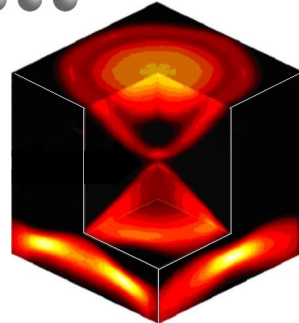
[2] Chen, Y. et al. *Science* **2010**, 329, 659–662. [3] Hou, Y. et al. *Science adv.* **2019**, 5, eaaw1874. [4] Otrokov, M. M. et al. *JETP Lett.* **2017**, 105, 297–302. [5] Otrokov, M. M. et al. *Nature* **2019**, 576, 416–422. [6] Rienks, E. D. et al. *Nature* **2019**, 576, 423–428. [7] Garnica, M. et al. *Npj Quant. Mat.* **2022**, 7, 1–9. [8] Grauer, S. et al. *PRB* **2015**, 92, 201304. [9] Pan, L. et al. *Science adv.* **2020**, 6, eaaz3595.



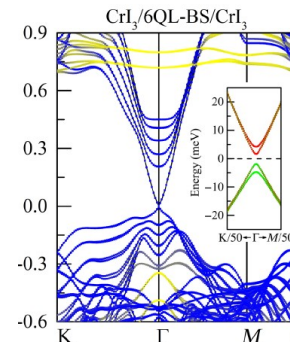
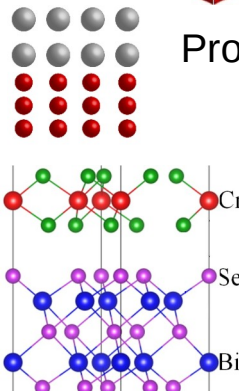
Introduction: magnetic TIs (MTIs)

- **Impurity magnetic doping**

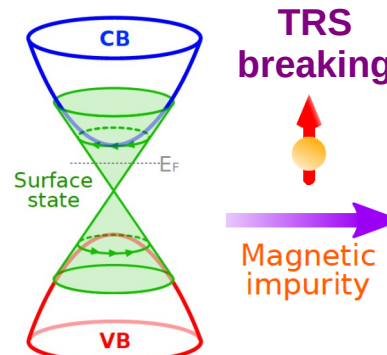
Substitutional or surface doping [2]



- **Proximity coupling [3]**

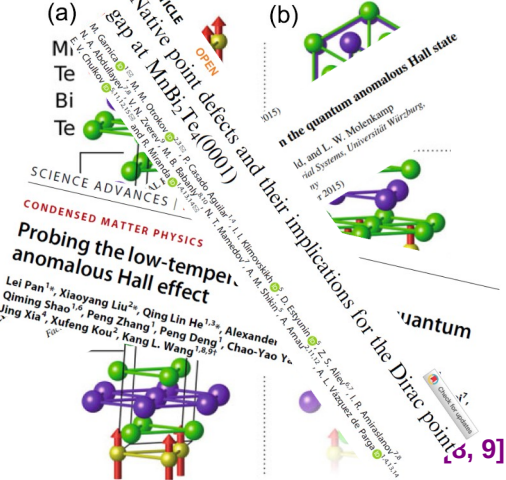
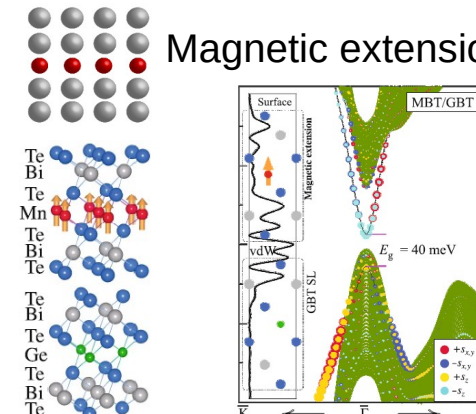
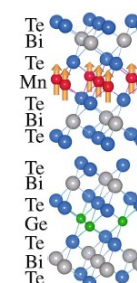
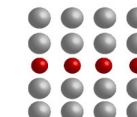


Massless Dirac fermions



Magnetic
impurity

Magnetic extension [4]



Prediction and observation of an antiferromagnetic topological insulator [5]

<https://doi.org/10.1038/s41586-019-1840-9>
Received: 20 September 2018
Accepted: 18 September 2019
Published online: 18 December 2019

Large magnetic gap at the Dirac point in Bi₂Te₃/MnBi₂Te₄ heterostructures [6]

<https://doi.org/10.1038/s41586-019-1826-7>
Received: 10 May 2018
Accepted: 18 October 2019
Published online: 18 December 2019

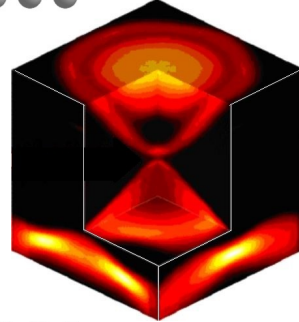
[2] Chen, Y. et al. *Science* **2010**, *329*, 659–662. [3] Hou, Y. et al. *Science adv.* **2019**, *5*, eaaw1874. [4] Otrokov, M. M. et al. *JETP Lett.* **2017**, *105*, 297–302. [5] Otrokov, M. M. et al. *Nature* **2019**, *576*, 416–422. [6] Rienks, E. D. et al. *Nature* **2019**, *576*, 423–428. [7] Garnica, M. et al. *Npj Quant. Mat.* **2022**, *7*, 1–9. [8] Grauer, S. et al. *PRB* **2015**, *92*, 201304. [9] Pan, L. et al. *Science adv.* **2020**, *6*, eaaz3595.



Introduction: magnetic TIs (MTIs)

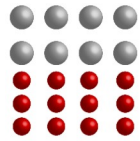
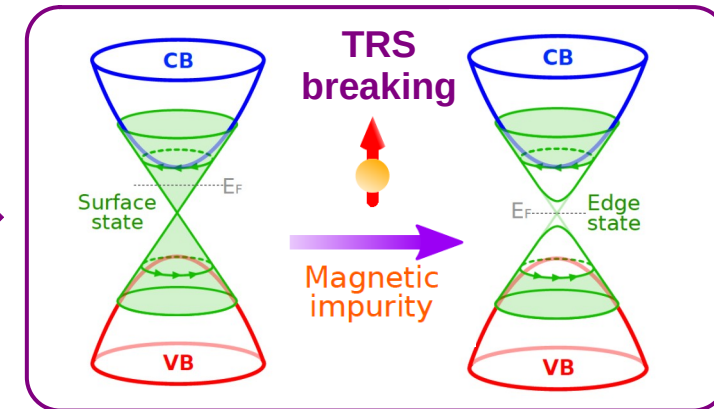
- **Impurity magnetic doping**

Substitutional or surface doping [2]

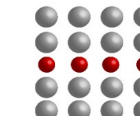
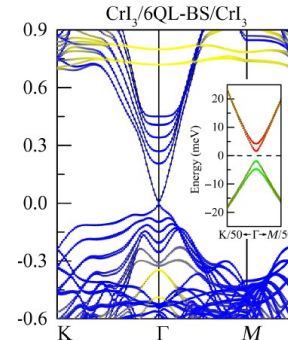
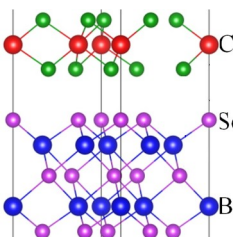


Massless Dirac fermions

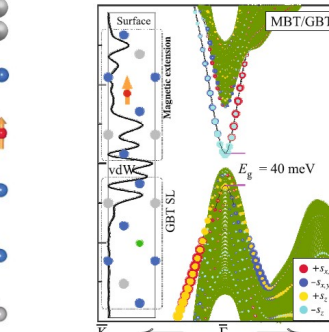
Massive Dirac fermions



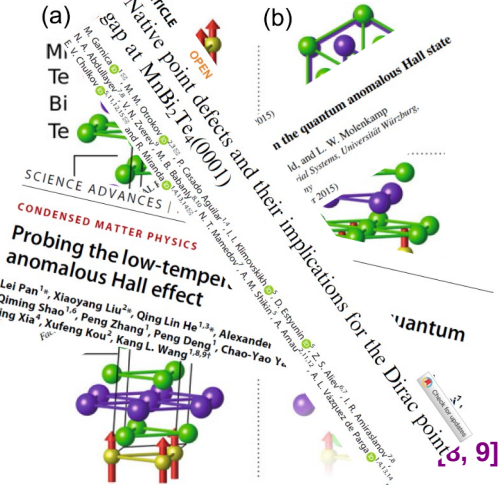
Proximity coupling [3]



Magnetic extension [4]



- [2] Chen, Y. et al. *Science* **2010**, 329, 659–662. [3] Hou, Y. et al. *Science adv.* **2019**, 5, eaaw1874. [4] Otrokov, M. M. et al. *JETP Lett.* **2017**, 105, 297–302. [5] Otrokov, M. M. et al. *Nature* **2019**, 576, 416–422. [6] Rienks, E. D. et al. *Nature* **2019**, 576, 423–428. [7] Garnica, M. et al. *Npj Quant. Mat.* **2022**, 7, 1–9. [8] Grauer, S. et al. *PRB* **2015**, 92, 201304. [9] Pan, L. et al. *Science adv.* **2020**, 6, eaaz3595.



Prediction and observation of an antiferromagnetic topological insulator [5]

<https://doi.org/10.1038/s41586-019-1840-9>
Received: 20 September 2018
Accepted: 18 September 2019
Published online: 18 December 2019

M. M. Otrokov^{1,2,3*}, I. I. Klimovskikh⁴, H. Bentmann⁵, D. Estyunin¹, A. Zeugner⁶, Z. S. Aliev^{1,8}, S. Gaß⁷, A. U. B. Wolter⁷, A. V. Koroleva⁸, A. M. Shikin¹, M. Blanco-Rey^{3,9}, M. Hoffmann⁹, I. P. Rusinov¹⁰, A. Yu. Yuzovskaya^{11,12}, S. V. Eremeev^{12,13}, Yu. M. Koroteev^{12,13}, V. M. Kuznetsov¹³, F. Freysoldt¹⁴, J. Sánchez-Barriga¹⁴, I. R. Amiraslanov¹⁵, M. B. Babany¹⁵, N. T. Mamedov¹⁵, N. A. Abdullaev¹⁶, V. N. Zverev¹⁶, A. Alfonsov¹⁶, V. Kataev¹⁶, B. Büchner¹⁷, F. E. Schwegler¹⁸, S. Kumar¹⁹, A. Kimura¹⁹, L. Petaccia¹⁹, O. Di Santo¹⁹, R. C. Vidal¹⁹, S. Schatz²⁰, K. Küller²⁰, M. Ünzelmann²⁰, C. H. Min²⁰, Simon Moser²⁰, T. R. Peixoto²¹, F. Reinert²¹, A. Ernst^{12,22}, P. M. Echenique^{12,22}, A. Isaeva^{12,22} & E. V. Chulkov^{12,22}

E. D. L. Rienks^{1,2,3*}, S. Wimmer^{4,4}, J. Sánchez-Barriga^{1,4}, O. Caha^{3,4}, P. S. Mandal^{3,4}, J. Ruzicka⁴, A. Neff⁴, H. Steiner⁴, V. V. Volobuev^{4,13}, H. Grottel⁴, M. Albu¹⁴, G. Kothleitner¹⁵, J. Michalkova¹⁴, S. A. Khan¹⁴, J. Minár¹⁵, H. Ebert¹⁵, G. Bauer¹⁵, F. Freysoldt¹⁴, A. Varykhov¹⁴, O. Rader¹⁴ & G. Springholz¹⁴

<https://doi.org/10.1038/s41586-019-1826-7>
Received: 10 May 2018
Accepted: 18 October 2019
Published online: 18 December 2019



Introduction: surface magnetic doping: 3d magnetic impurities





Introduction: surface magnetic doping: 3d magnetic impurities

Growth
Doping

www.nanoscience.mdeia.org





Introduction: surface magnetic doping: 3d magnetic impurities

Growth



Doping





Introduction: surface magnetic doping: 3d magnetic impurities

Growth
Doping



[10]

Limiting dopants to TSSs most sensitive regions
Maximizing magnetic anisotropy by the lower coordination symmetry



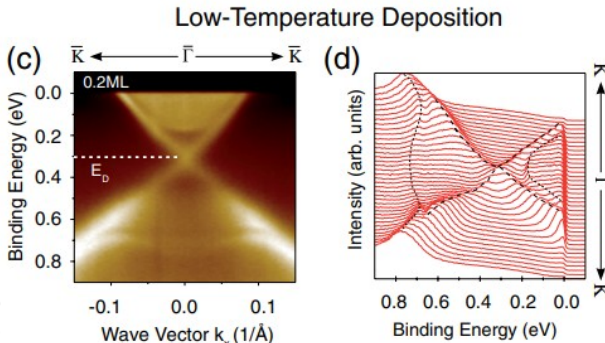
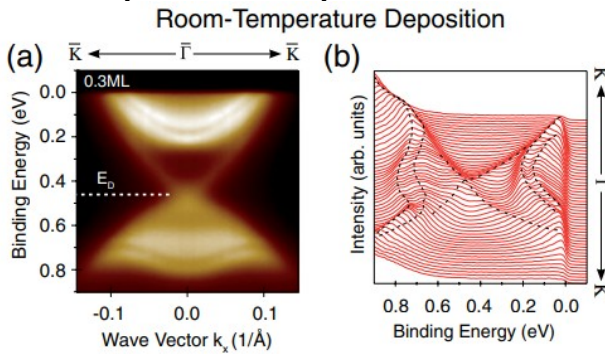
Introduction: surface magnetic doping: 3d magnetic impurities

Growth
Doping



Limiting dopants to TSSs most sensitive regions
Maximizing magnetic anisotropy by the lower coordination symmetry

Multiple adsorption sites [11]



[10] Gambardella, P. et al. Science, 2003, 300(5622), 1130-1133. [11] Scholz, M. R. et al. Physical Review Letters, 2012, 108(25), 256810.



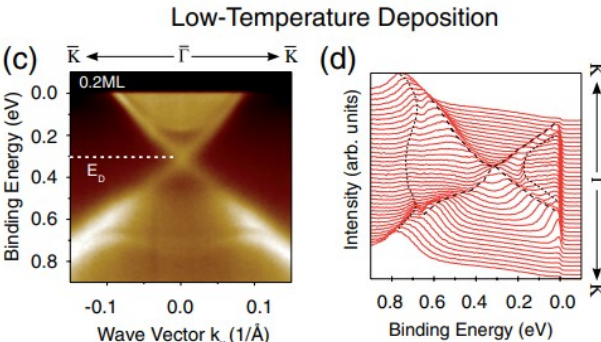
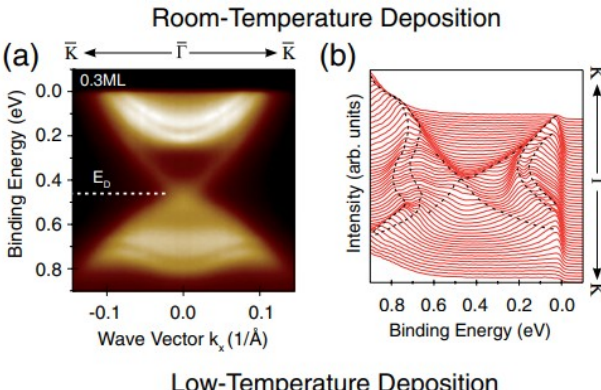
Introduction: surface magnetic doping: 3d magnetic impurities

Growth
Doping



Limiting dopants to TSSs most sensitive regions
Maximizing magnetic anisotropy by the lower coordination symmetry

Multiple adsorption sites [11]



[12] Gambardella, P. et al. *Science*, **2003**, 300(5622), 1130-1133. [11] Scholz, M. R. et al. *Physical Review Letters*, **2012**, 108(25), 256810. [12] Honolka, J. et al. *Physical review letters*, **2012**, 108(25), 256811.

Strong surface relaxations [12]

PHYSICAL REVIEW LETTERS

In-Plane Magnetic Anisotropy of Fe Atoms on $\text{Bi}_2\text{Se}_3(111)$

J. Honolka,^{1,*} A. A. Khajetoorians,^{2,†} V. Sessi,³ T. O. Wehling,^{4,5,6} S. Stepanow,¹ J.-L. Mi,⁷ B. B. Iversen,⁷ T. Schlenk,² J. Wiebe,² N. B. Brookes,³ A. I. Lichtenstein,⁴ Ph. Hofmann,⁸ K. Kern,^{1,9} and R. Wiesendanger²

¹Max-Planck-Institut für Festkörperforschung, Heisenbergstrasse 1, 70569 Stuttgart, Germany

²Institute for Applied Physics, Universität Hamburg, D-20355 Hamburg, Germany

³European Synchrotron Radiation Facility, BP 220, F-38043 Grenoble, France

⁴I. Institut für Theoretische Physik, Universität Hamburg, D-20355 Hamburg, Germany

⁵Institut für Theoretische Physik, Universität Bremen, Otto-Hahn-Allee 1, D-28359 Bremen, Germany

⁶Bremen Center for Computational Materials Science, Universität Bremen, Am Fallturm 1a, D-28359 Bremen, Germany

⁷Center for Materials Crystallography, Department of Chemistry, Interdisciplinary Nanoscience Center, Aarhus University, 8000 Aarhus C, Denmark

⁸Department of Physics and Astronomy, Interdisciplinary Nanoscience Center, Aarhus University, 8000 Aarhus C, Denmark

⁹Institut de Physique de la Matière Condensée, Ecole Polytechnique Fédérale de Lausanne, CH-1015 Lausanne, Switzerland

(Received 20 December 2011; published 22 June 2012)

The robustness of the gapless topological surface state hosted by a 3D topological insulator against perturbations of magnetic origin has been the focus of recent investigations. We present a comprehensive study of the magnetic properties of Fe impurities on the prototypical 3D topological insulator Bi_2Se_3 using local low-temperature scanning tunneling spectroscopy and integral x-ray magnetic circular dichroism techniques. Single Fe adatoms on the Bi_2Se_3 surface, in the coverage range $\approx 1\%$ of a monolayer, are heavily relaxed into the surface and exhibit a magnetic easy axis within the surface plane, contrary to what was assumed in recent investigations on the supposed opening of a gap. Using *ab initio* approaches, we demonstrate that an in-plane easy axis arises from the combination of the crystal field and dynamic hybridization effects.

DOI: [10.1103/PhysRevLett.108.256811](https://doi.org/10.1103/PhysRevLett.108.256811)

PACS numbers: 73.20.At, 68.37.Ef, 71.15.Mb, 78.70.Dm



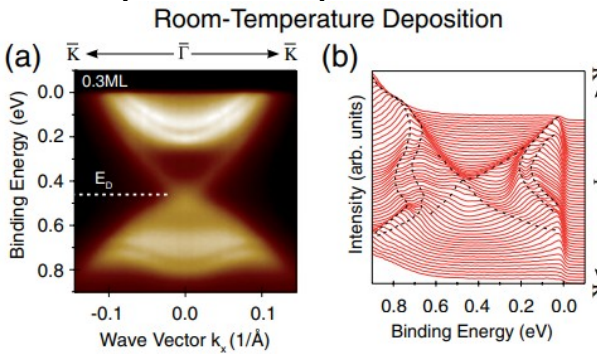
Introduction: surface magnetic doping: 3d magnetic impurities

Growth
Doping



Limiting dopants to TSSs most sensitive regions
Maximizing magnetic anisotropy by the lower coordination symmetry

Multiple adsorption sites [11]



Strong surface relaxations [12]

PHYSICAL REVIEW LETTERS

In-Plane Magnetic Anisotropy of Fe Atoms on $\text{Bi}_2\text{Se}_3(111)$

J. Honolka,^{1,*} A. A. Khajetoorians,^{2,†} V. Sessi,³ T. O. Wehling,^{4,5,6} S. Stepanow,¹ J.-L. Mi,⁷ B. B. Iversen,⁷ T. Schlenk,² J. Wiebe,² N. B. Brookes,³ A. I. Lichtenstein,⁴ Ph. Hofmann,⁸ K. Kern,^{1,9} and R. Wiesendanger²

¹Max-Planck-Institut für Festkörperforschung, Heisenbergstrasse 1, 70569 Stuttgart, Germany

²Institute for Applied Physics, Universität Hamburg, B220, F-38043 Grenoble, France

³European Synchrotron Radiation Facility, BP 220, F-38043 Grenoble, France

⁴Institut für Theoretische Physik, Universität Bremen, Otto-Hahn-Allee 1, D-28359 Bremen, Germany

⁵Bremen Center for Computational Materials Science, Otto-Hahn-Allee 1a, D-28359 Bremen, Germany

⁶Center for Materials Crystallography, Department of Chemistry, Interdisciplinary Nanoscience Center,

Aarhus University, 8000 Aarhus C, Denmark

⁷Department of Physics and Astronomy, Interdisciplinary Nanoscience Center, Aarhus University, 8000 Aarhus C, Denmark

⁸Institut de Physique de la Matière Condensée, Ecole Polytechnique Fédérale de Lausanne, CH-1015 Lausanne, Switzerland

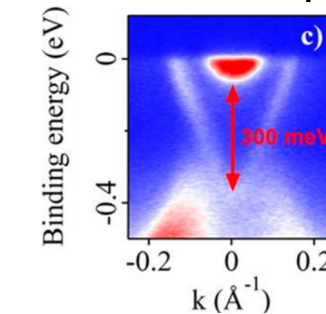
(Received 20 December 2011; published 22 June 2012)

The robustness of the gapless topological surface state hosted by a 3D topological insulator against perturbations of magnetic origin has been the focus of recent investigations. We present a comprehensive study of the magnetic properties of Fe impurities on the prototypical 3D topological insulator Bi_2Se_3 using local low-temperature scanning tunneling spectroscopy and integral x-ray magnetic circular dichroism techniques. Single Fe adatoms on the Bi_2Se_3 surface, in the coverage range $\approx 1\%$ of a monolayer, are heavily relaxed into the surface and exhibit a magnetic easy axis within the surface plane, contrary to what was assumed in recent investigations on the supposed opening of a gap. Using *ab initio* approaches, we demonstrate that an in-plane easy axis arises from the combination of the crystal field and dynamic hybridization effects.

DOI: 10.1103/PhysRevLett.108.256811

PACS numbers: 73.20.At, 68.37.Ef, 71.15.Mb, 78.70.Dm

Bulk states doping [13]



THE JOURNAL OF
PHYSICAL CHEMISTRY C

pubs.acs.org/JPCC

Observation of Distinct Bulk and Surface Chemical Environments in a Topological Insulator under Magnetic Doping

Ivana Voborník,^{*,†,‡} Giancarlo Panaccione,^{*,†,‡} Jun Fujii,[†] Zhi-Huai Zhu,[†] Francesco Offi,[§] Benjamin R. Salles,^{*,△} Francesco Borgatti,[†] Piero Tortella,[†] Jean Pascal Rueff,[†] Denis Céolin,[†] Alberto Artioli,[†] Manju Unnikrishnan,[†] Giorgio Levy,^{†,○} Massimiliano Marangolo,[●] Mamoudou Eddrief,[○] Damjan Krizmančič,[○] Huiven Jia,[○] Andrea Damascelli,^{○,‡} Gerrit van der Laan,[○] Russell G. Eggleton,[○] and Robert J. Cava[○]

^{*}Istituto Officina dei Materiali (IOM)-CNR, Laboratorio TASC, Area Science Park, SS14, Km 163.5, I-34149 Trieste, Italy

[†]Department of Physics & Astronomy, University of British Columbia, Vancouver, British Columbia V6T 1Z1, Canada

[‡]Dipartimento di Scienze, Università di Roma Tre, I-00146 Rome, Italy

[○]SMN-CNR, via Gobetti 101, I-40129 Bologna, Italy

[○]Synchrotron SOLEIL, L'Orme des Merisier, BP 48, Saint-Aubin, 91192 Gif sur Yvette, France

[○]Laboratoire de Chimie Physique – Matière et Rayonnement, Université Pierre et Marie Curie, CNRS, 11 rue Pierre et Marie Curie, F-75005 Paris, France

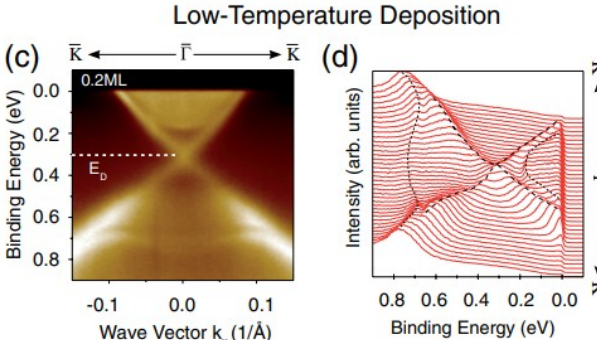
[○]International Institute of Nanosciences de Paris, UPMC-CNRS UMR 7586, 4 place Jussieu, 75232 Paris Cedex 5, France

[○]Department of Chemistry, Princeton University, Princeton, New Jersey 08544, United States

[○]Diamond Light Source, Chilton, Didcot, Oxfordshire OX11 0DE, United Kingdom

[○]Department of Chemistry, Inorganic Chemistry Laboratory, University of Oxford, South Parks Road, Oxford OX1 3QR, United Kingdom

[○]International Centre for Theoretical Physics, Strada Costiera 11, 34100 Trieste, Italy



[10] Gambardella, P. et al. *Science*, **2003**, 300(5622), 1130-1133. [11] Scholz, M. R. et al. *Physical Review Letters*, **2012**, 108(25), 256810. [12] Honolka, J. et al. *Physical review letters*, **2012**, 108(25), 256811. [13] Voborník, I. Et al. *The Journal of Physical Chemistry C*, **2014**, 118(23), 12333-12339.



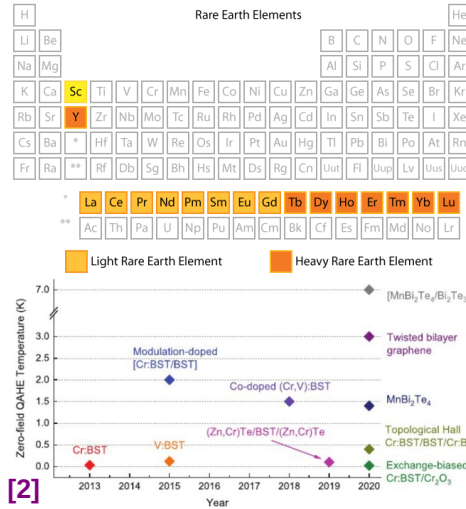


Introduction: rare-earth (RE) surface magnetic doping





Introduction: rare-earth (RE) surface magnetic doping

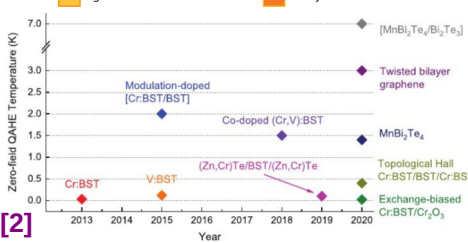
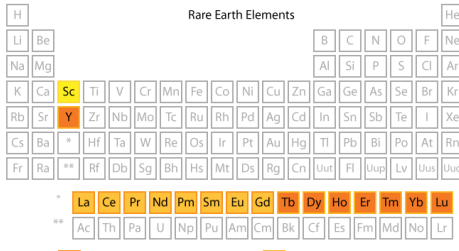


- **Larger size** → prevents from substitutional sites → reduced the multiplicity of adsorption configurations [14]

[14] L. B. Abdalla, et al. PRB, 2013, 88, 045312.



Introduction: rare-earth (RE) surface magnetic doping

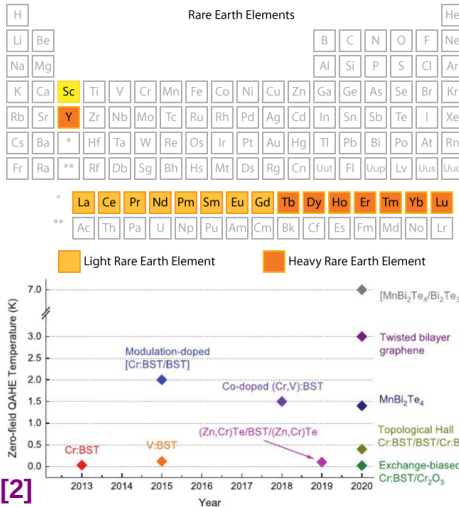


- Larger size → prevents from substitutional sites → reduced the multiplicity of adsorption configurations [14]
- Unpaired 4f electrons → **large magnetic moments** → enhanced magnetic anisotropy [15] and allow a lower doping concentration [16]

[14] L. B. Abdalla, et al. PRB, **2013**, 88, 045312. [15] Jensen, J., & Mackintosh, A. R. (**1991**). Rare earth magnetism (p. 312). Oxford: Clarendon Press. [16] Harrison, S. E. et al. JoP: Cond. Matt., **2015**, 27(24), 245602.



Introduction: rare-earth (RE) surface magnetic doping

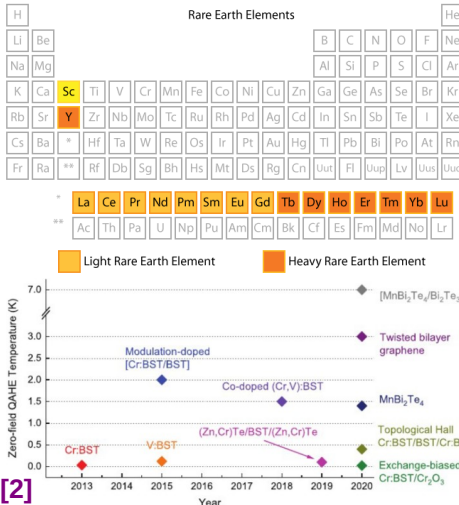


- Larger size → prevents from substitutional sites → reduced the multiplicity of adsorption configurations [14]
- Unpaired 4f electrons → large magnetic moments → enhanced magnetic anisotropy [15] and allow a lower doping concentration [16]
- Curie temperatures as high as 80K [17]

[14] L. B. Abdalla, et al. PRB, **2013**, 88, 045312. [15] Jensen, J., & Mackintosh, A. R. (1991). Rare earth magnetism (p. 312). Oxford: Clarendon Press. [16] Harrison, S. E. et al. JoP: Cond. Matt., **2015**, 27(24), 245602. [17] Omarza M. er al. Nano Lett. **2016**, 16, 7, 4230–4235.



Introduction: rare-earth (RE) surface magnetic doping

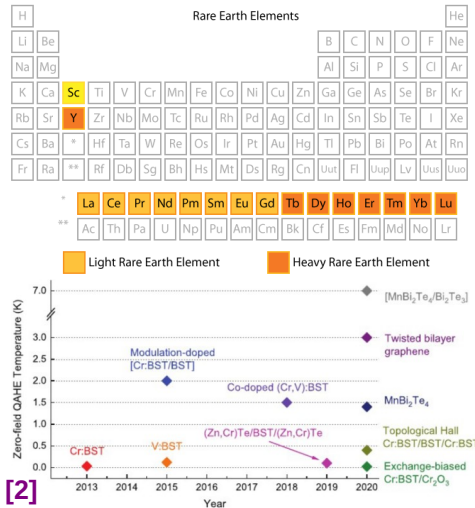


- Larger size → prevents from substitutional sites → reduced the multiplicity of adsorption configurations [14]
- Unpaired 4f electrons → large magnetic moments → enhanced magnetic anisotropy [15] and allow a lower doping concentration [16]
- Curie temperatures as high as 80K [17]
- **RE substitutional bulk doping:** Eu [18], Gd [19], Ho [20] and Dy [21] on Bi₂Te₃.

[14] L. B. Abdalla, et al. PRB, **2013**, 88, 045312. [15] Jensen, J., & Mackintosh, A. R. (1991). Rare earth magnetism (p. 312). Oxford: Clarendon Press. [16] Harrison, S. E. et al. JoP: Cond. Matt., **2015**, 27(24), 245602. [17] Omarza M. er al. Nano Lett. **2016**, 16, 7, 4230–4235. [18] Celso I. Fornari et al. J. Phys. Chem. C **2020**, 124, 29, 16048–16057. [19] Kim, J. et al. Sci Rep 5, 2015, 10309. [20] Hesjedal T. et al. physica status solidi (a), **2019**, 216(8), 1800726. [21] S. Harrison et al. J. Phys.: Condens. Matter, **2015**, 27 245602



Introduction: rare-earth (RE) surface magnetic doping

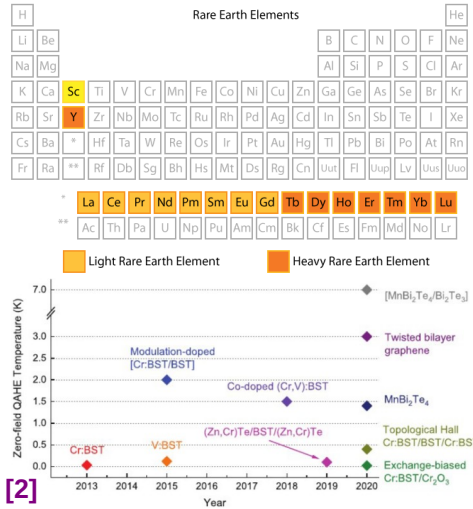


- Larger size → prevents from substitutional sites → reduced the multiplicity of adsorption configurations [14]
- Unpaired 4f electrons → large magnetic moments → enhanced magnetic anisotropy [15] and allow a lower doping concentration [16]
- Curie temperatures as high as 80K [17]
- **RE substitutional bulk doping:** Eu [18], Gd [19], Ho [20] and Dy [21] on Bi₂Te₃.
- **Bandgap opening** only for certain Dy concentrations [22]

[14] L. B. Abdalla, et al. PRB, **2013**, 88, 045312. [15] Jensen, J., & Mackintosh, A. R. (1991). Rare earth magnetism (p. 312). Oxford: Clarendon Press. [16] Harrison, S. E. et al. JoP: Cond. Matt., **2015**, 27(24), 245602. [17] Omarza M. er al. Nano Lett. **2016**, 16, 7, 4230–4235. [18] Celso I. Fornari et al. J. Phys. Chem. C **2020**, 124, 29, 16048–16057. [19] Kim, J. et al. Sci Rep 5, 2015, 10309. [20] Hesjedal T. et al. physica status solidi (a), **2019**, 216(8), 1800726. [21] S. Harrison et al. J. Phys.: Condens. Matter, **2015**, 27 245602. [22] S. Harrison et al. Sci Rep 5, **2015**, 15767.



Introduction: rare-earth (RE) surface magnetic doping



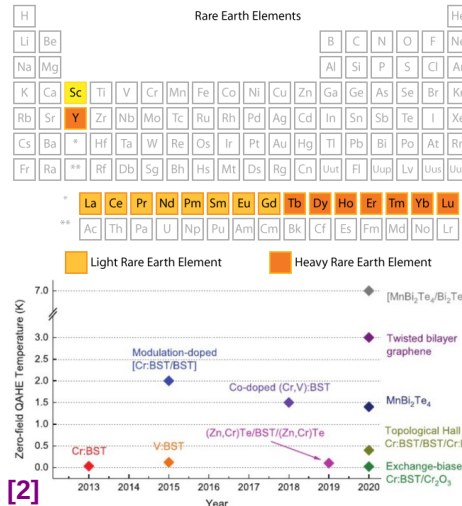
Magnetic order in MTIs

- Larger size → prevents from substitutional sites → reduced the multiplicity of adsorption configurations [14]
- Unpaired 4f electrons → large magnetic moments → enhanced magnetic anisotropy [15] and allow a lower doping concentration [16]
- Curie temperatures as high as 80K [17]
- RE substitutional bulk doping: Eu [18], Gd [19], Ho [20] and Dy [21] on Bi₂Te₃.
- Bandgap opening only for certain Dy concentrations [22]

[14] L. B. Abdalla, et al. PRB, **2013**, 88, 045312. [15] Jensen, J., & Mackintosh, A. R. (1991). Rare earth magnetism (p. 312). Oxford: Clarendon Press. [16] Harrison, S. E. et al. JoP: Cond. Matt., **2015**, 27(24), 245602. [17] Omarza M. er al. Nano Lett. **2016**, 16, 7, 4230–4235. [18] Celso I. Fornari et al. J. Phys. Chem. C **2020**, 124, 29, 16048–16057. [19] Kim, J. et al. Sci Rep 5, 2015, 10309. [20] Hesjedal T. et al. physica status solidi (a), **2019**, 216(8), 1800726. [21] S. Harrison et al. J. Phys.: Condens. Matter, **2015**, 27 245602. [22] S. Harrison et al. Sci Rep 5, **2015**, 15767.

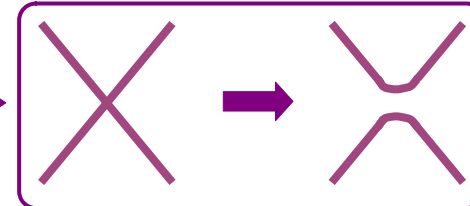


Introduction: rare-earth (RE) surface magnetic doping



Magnetic order in MTIs

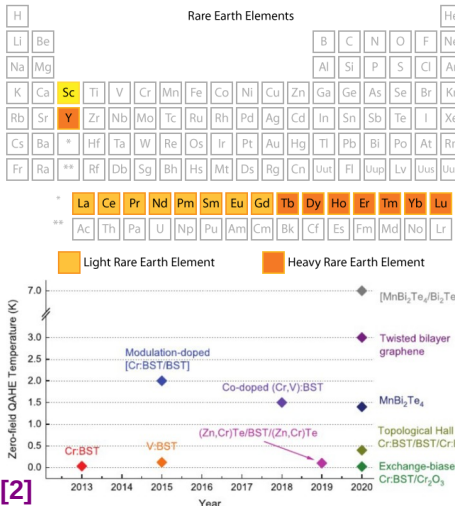
[23, 24]



[14] L. B. Abdalla, et al. PRB, **2013**, 88, 045312. [15] Jensen, J., & Mackintosh, A. R. (1991). Rare earth magnetism (p. 312). Oxford: Clarendon Press. [16] Harrison, S. E. et al. JoP: Cond. Matt., **2015**, 27(24), 245602. [17] Omarza M. er al. Nano Lett. **2016**, 16, 7, 4230–4235. [18] Celso I. Formari et al. J. Phys. Chem. C **2020**, 124, 29, 16048–16057. [19] Kim, J. et al. Sci Rep 5, 2015, 10309. [20] Hesjedal T. et al. physica status solidi (a), **2019**, 216(8), 1800726. [21] S. Harrison et al. J. Phys.: Condens. Matter, **2015**, 27 245602. [22] S. Harrison et al. Sci Rep 5, **2015**, 15767. [23] H.Tanet al. Phys. Rev. Materials 6, **2022**, 104204 . [24] G. Naselli et al. Phys. Rev. Research 4, **2022**, 033198

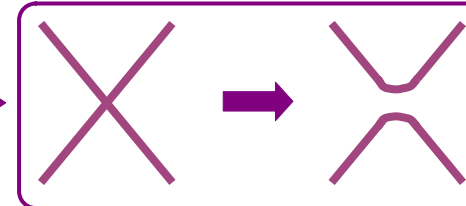


Introduction: rare-earth (RE) surface magnetic doping



Magnetic order in MTIs

[23, 24]



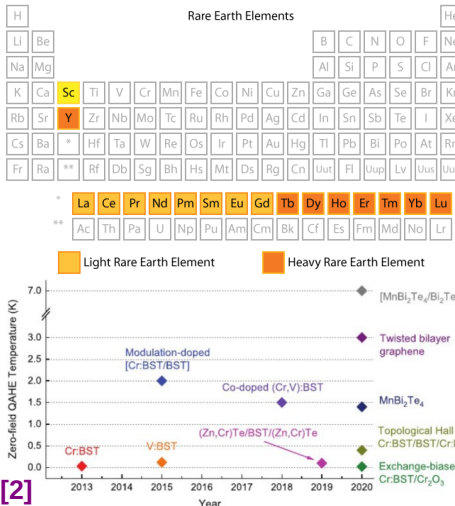
+



[14] L. B. Abdalla, et al. PRB, **2013**, 88, 045312. [15] Jensen, J., & Mackintosh, A. R. (1991). Rare earth magnetism (p. 312). Oxford: Clarendon Press. [16] Harrison, S. E. et al. JoP: Cond. Matt., **2015**, 27(24), 245602. [17] Omarza M. er al. Nano Lett. **2016**, 16, 7, 4230–4235. [18] Celso I. Fornari et al. J. Phys. Chem. C **2020**, 124, 29, 16048–16057. [19] Kim, J. et al. Sci Rep 5, 2015, 10309. [20] Hesjedal T. et al. physica status solidi (a), **2019**, 216(8), 1800726. [21] S. Harrison et al. J. Phys.: Condens. Matter, **2015**, 27 245602. [22] S. Harrison et al. Sci Rep 5, **2015**, 15767. [23] H.Tanet al. Phys. Rev. Materials 6, **2022**, 104204 . [24] G. Naselli et al. Phys. Rev. Research 4, **2022**, 033198

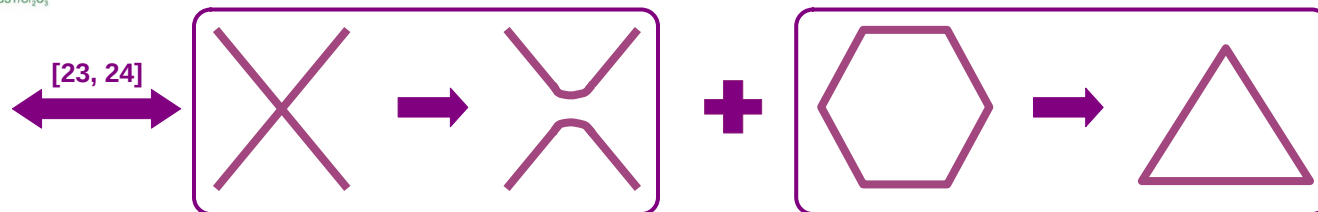


Introduction: rare-earth (RE) surface magnetic doping



Magnetic order in MTIs

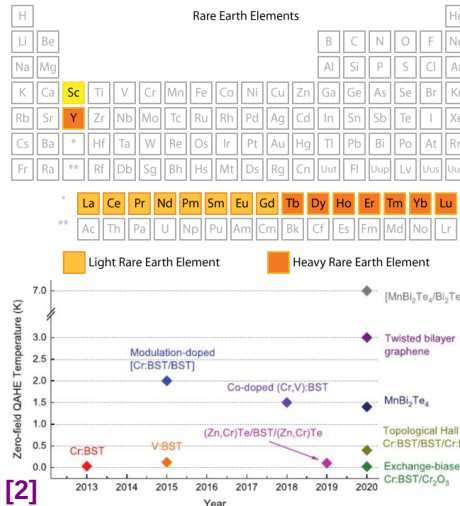
- Larger size → prevents from substitutional sites → reduced the multiplicity of adsorption configurations [14]
- Unpaired 4f electrons → large magnetic moments → enhanced magnetic anisotropy [15] and allow a lower doping concentration [16]
- Curie temperatures as high as 80K [17]
- RE substitutional bulk doping: Eu [18], Gd [19], Ho [20] and Dy [21] on Bi₂Te₃.
- Bandgap opening only for certain Dy concentrations [22]



[14] L. B. Abdalla, et al. PRB, **2013**, 88, 045312. [15] Jensen, J., & Mackintosh, A. R. (1991). Rare earth magnetism (p. 312). Oxford: Clarendon Press. [16] Harrison, S. E. et al. JoP: Cond. Matt., **2015**, 27(24), 245602. [17] Omarza M. er al. Nano Lett. **2016**, 16, 7, 4230–4235. [18] Celso I. Fornari et al. J. Phys. Chem. C **2020**, 124, 29, 16048–16057. [19] Kim, J. et al. Sci Rep 5, 2015, 10309. [20] Hesjedal T. et al. physica status solidi (a), **2019**, 216(8), 1800726. [21] S. Harrison et al. J. Phys.: Condens. Matter, **2015**, 27 245602. [22] S. Harrison et al. Sci Rep 5, **2015**, 15767. [23] H.Tanet al. Phys. Rev. Materials 6, **2022**, 104204 . [24] G. Naselli et al. Phys. Rev. Research 4, **2022**, 033198

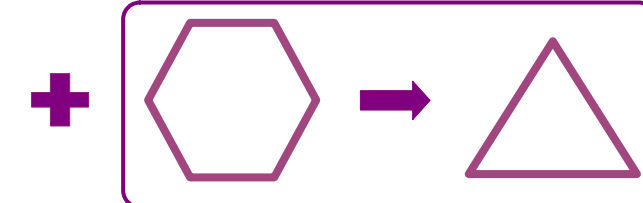
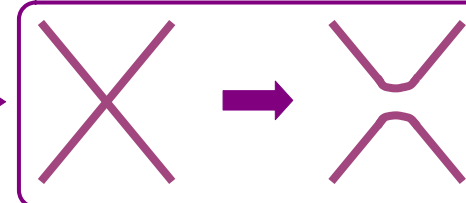


Introduction: rare-earth (RE) surface magnetic doping



Magnetic order in MTIs

[23, 24]



We experimentally report for the first time and theoretically demonstrate such effects on Er-doped Bi₂Se₂Te (BST), along with the tunability of the E_F as a function of the RE coverage, fulfilling the two prerequisites for the realization of the QAHE

[14] L. B. Abdalla, et al. PRB, **2013**, 88, 045312. [15] Jensen, J., & Mackintosh, A. R. (1991). Rare earth magnetism (p. 312). Oxford: Clarendon Press. [16] Harrison, S. E. et al. JoP: Cond. Matt., **2015**, 27(24), 245602. [17] Omarza M. er al. Nano Lett. **2016**, 16, 7, 4230–4235. [18] Celso I. Formari et al. J. Phys. Chem. C **2020**, 124, 29, 16048–16057. [19] Kim, J. et al. Sci Rep 5, 2015, 10309. [20] Hesjedal T. et al. physica status solidi (a), **2019**, 216(8), 1800726. [21] S. Harrison et al. J. Phys.: Condens. Matter, **2015**, 27 245602. [22] S. Harrison et al. Sci Rep 5, **2015**, 15767. [23] H.Tanet al. Phys. Rev. Materials 6, **2022**, 104204 . [24] G. Naselli et al. Phys. Rev. Research 4, **2022**, 033198



Experimental methods





Experimental methods



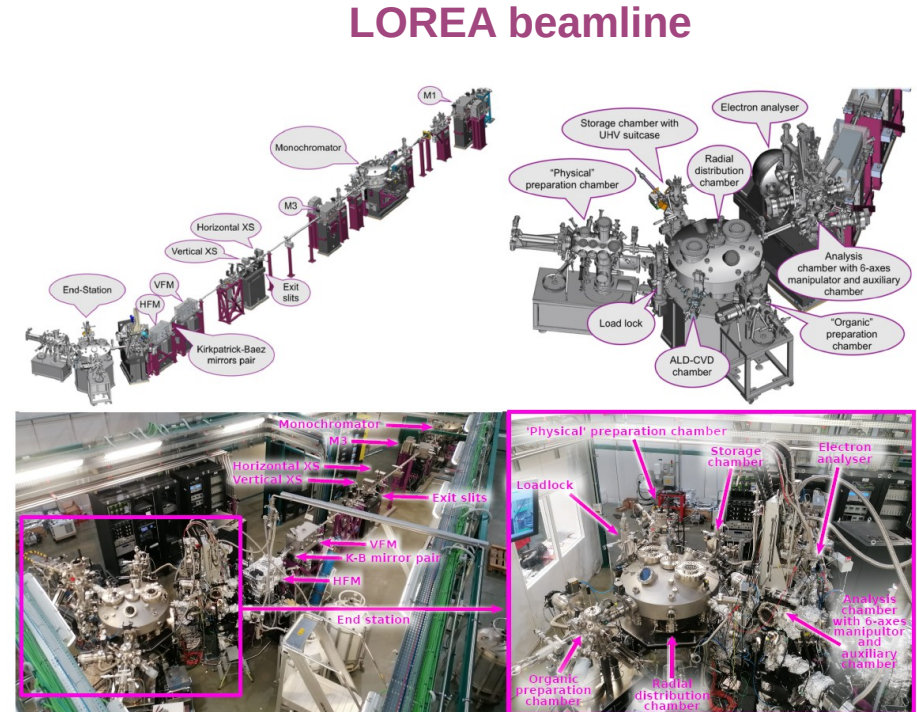


Experimental methods





Experimental methods



Analyser:

- MBS A-1 hemispherical analyser.
- Resolution better than 1 meV and 0.1° .
- Fast Fermi Surface mapping mode.
- Recently added spin detector.

Cryo-manipulator:

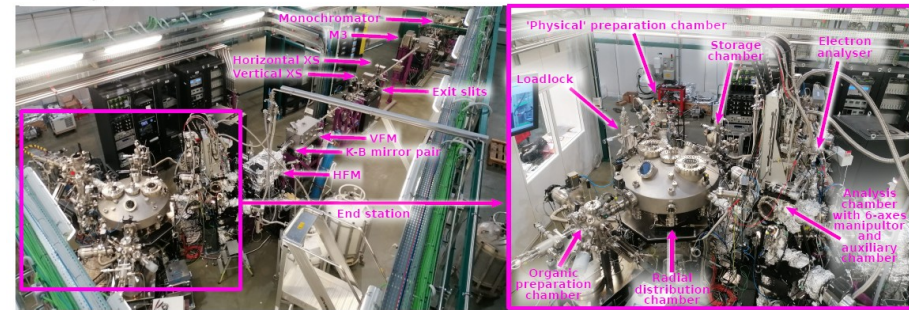
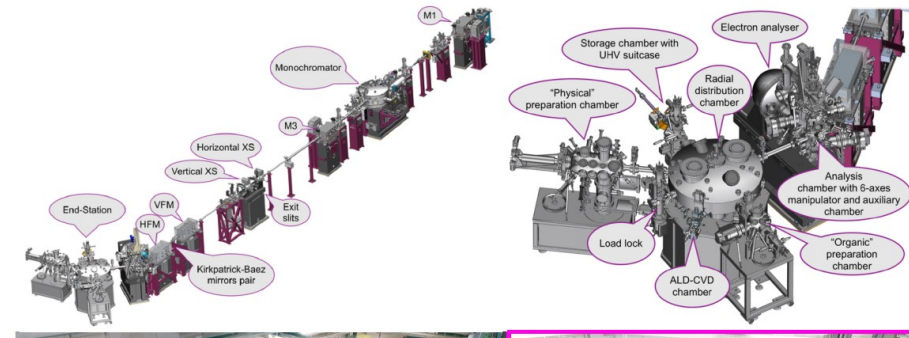
- 6 axes of movement.
- Allows reaching temperatures lower than 7.5 K .



Experimental methods



LOREA beamline



Analyser:

- MBS A-1 hemispherical analyser.
- Resolution better than -1 meV and 0.1° .
- Fast Fermi Surface mapping mode.
- Recently added spin detector.

Cryo-manipulator:

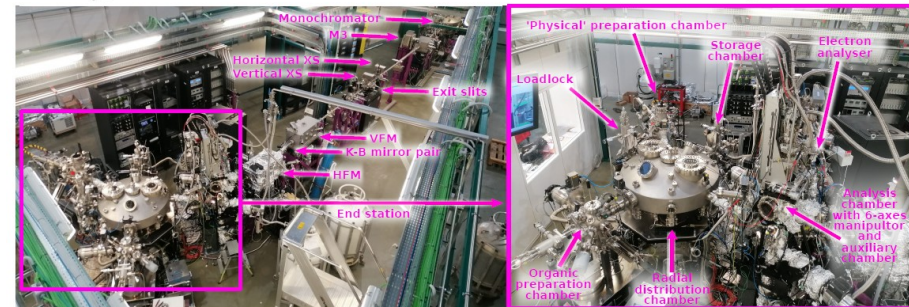
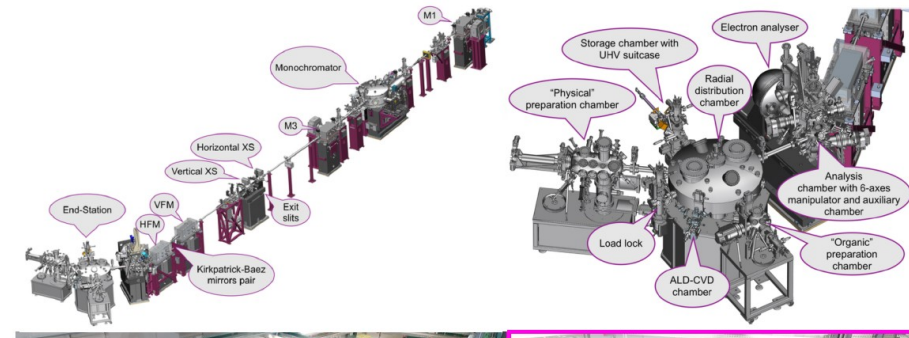
- 6 axes of movement.
- Allows reaching temperatures lower than 7.5 K .



Experimental methods



LOREA beamline



Analyser:

- MBS A-1 hemispherical analyser.
- Resolution better than -1 meV and 0.1° .
- Fast Fermi Surface mapping mode.
- Recently added spin detector.

Cryo-manipulator:

- 6 axes of movement.
- Allows reaching temperatures lower than 7.5 K .





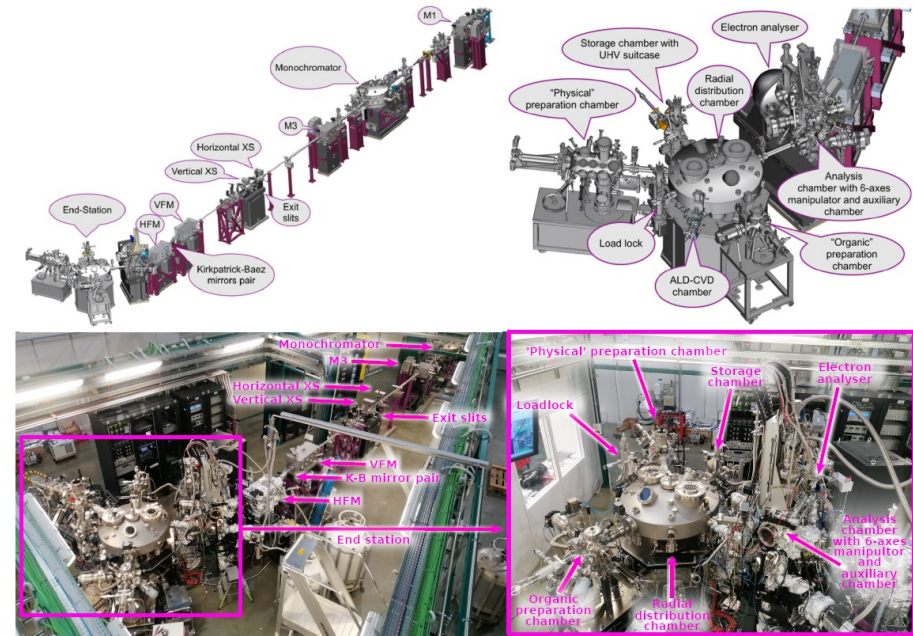
Experimental methods



- Bulk single crystal
- Er impurities deposited by means of an e-beam evaporator.
- XPS and ARPES performed at a T = 15 K
- Exfoliated in-situ (UHV) at T = 15 K
- Linear horizontal polarization $h\nu = 100$ (XPS) and 52 (ARPES) eV

Muñiz Cano, B., et al. *Nano Lett.* **2023**, 23, 13, 6249–6258

LOREA beamline



Analyser:

- MBS A-1 hemispherical analyser.
- Resolution better than -1 meV and 0.1°.
- Fast Fermi Surface mapping mode.
- Recently added spin detector.

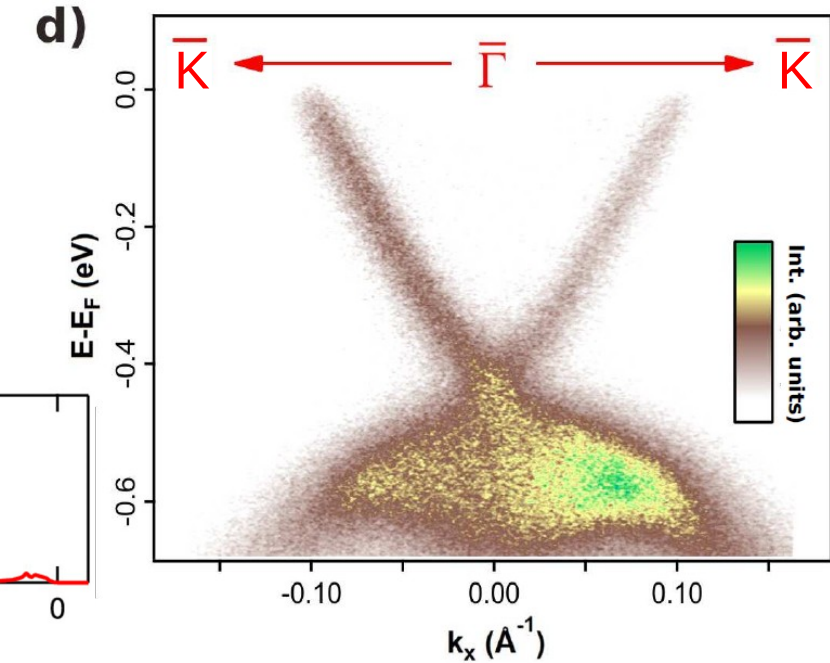
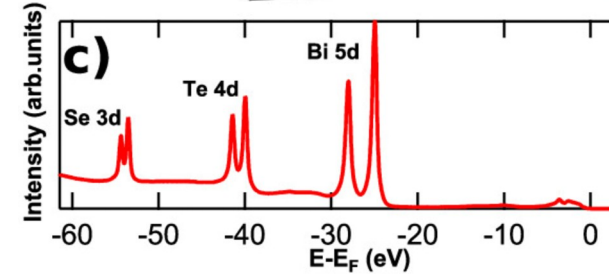
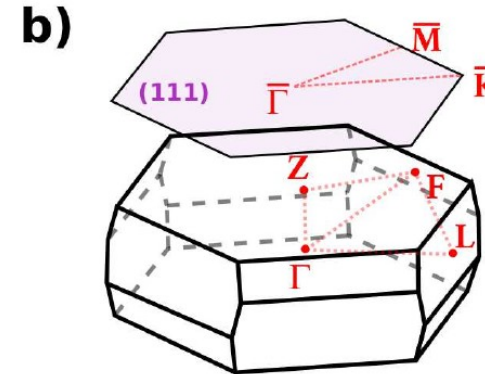
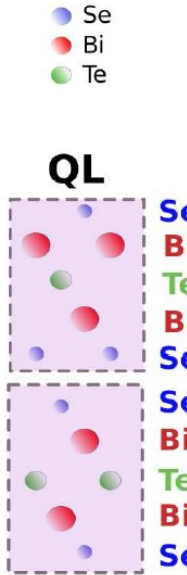
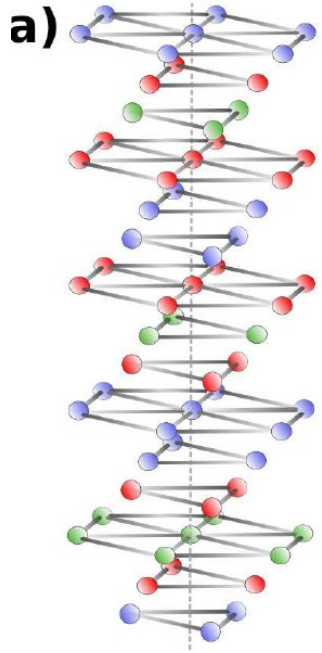
Cryo-manipulator:

- 6 axes of movement.
- Allows reaching temperatures lower than 7.5 K.



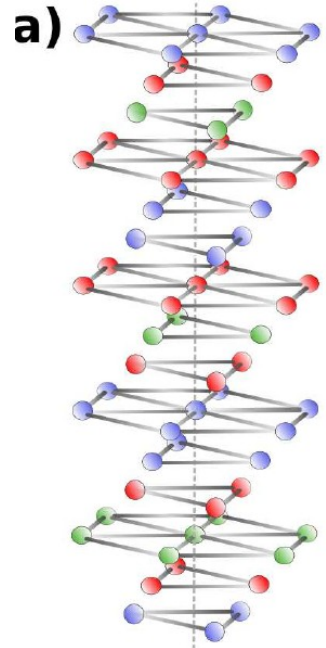


Results: pristine $\text{Bi}_2\text{Se}_2\text{Te}$



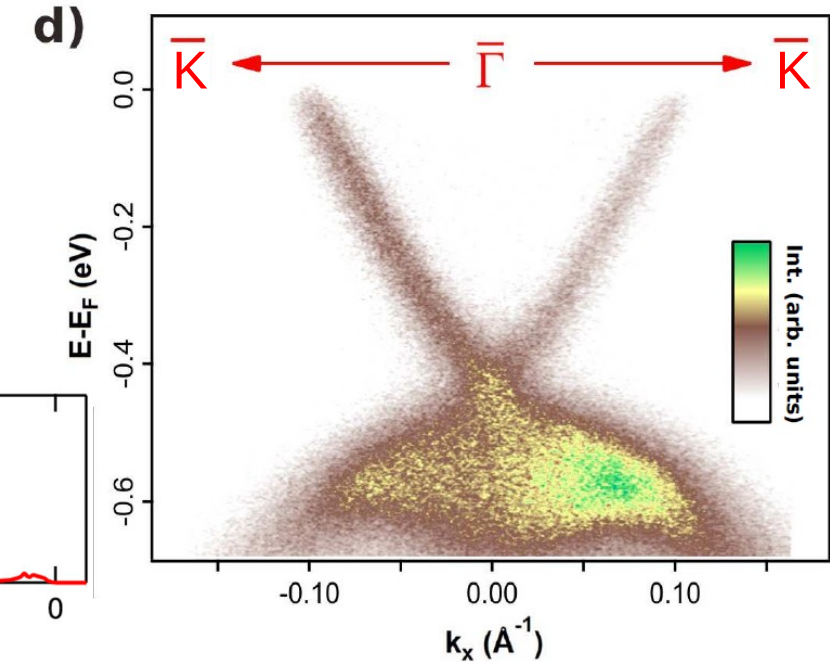
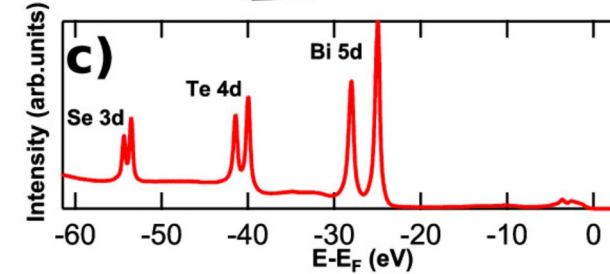
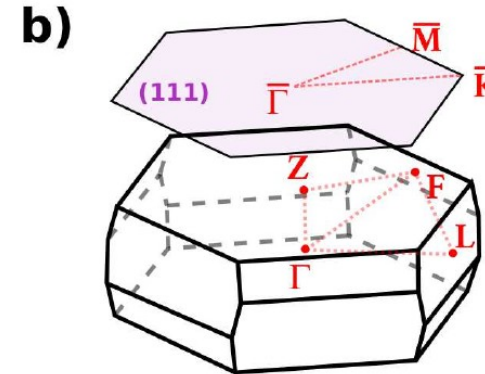


Results: pristine Bi₂Se₂Te



QL

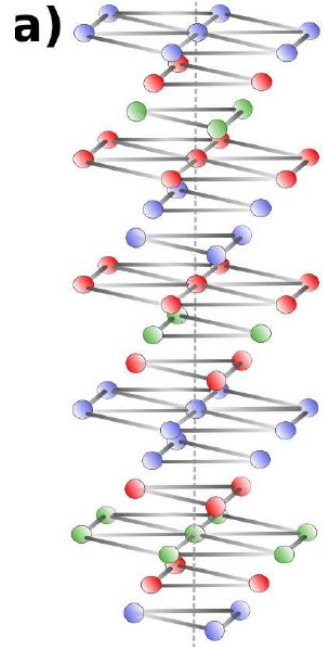
Se	Bi	Te
Bi	Se	Se
Se	Bi	Te
Bi	Se	Se
Se	Bi	Te
Bi	Se	Se



- 3D quintuple layer crystal structure.

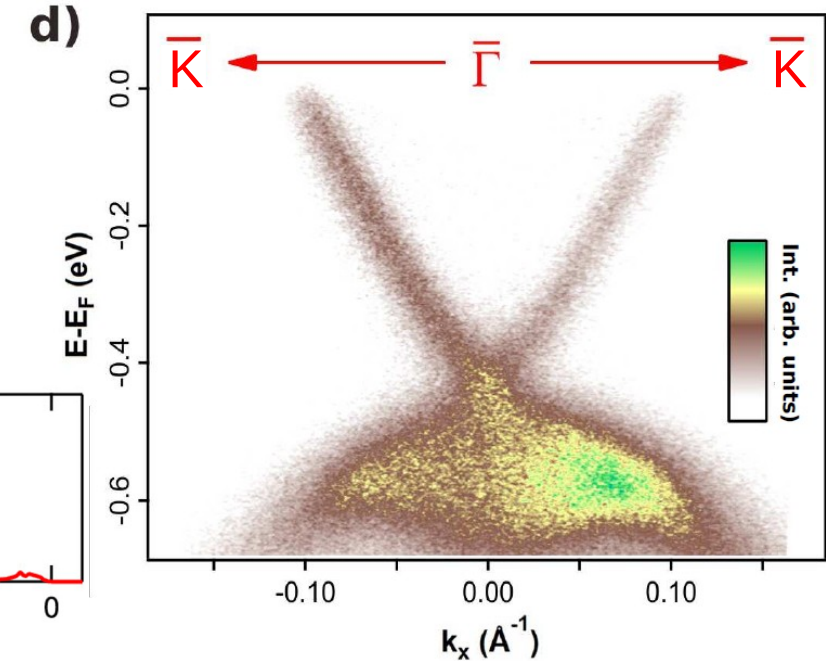
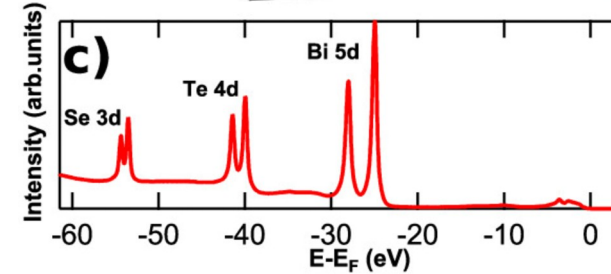
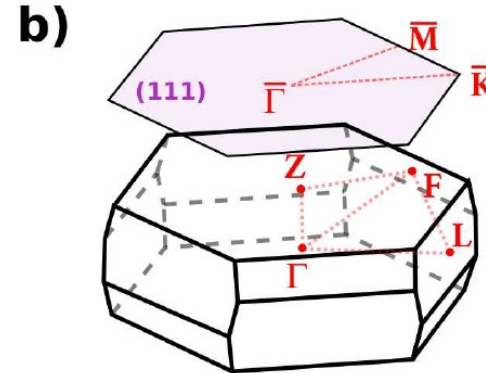


Results: pristine Bi₂Se₂Te



QL

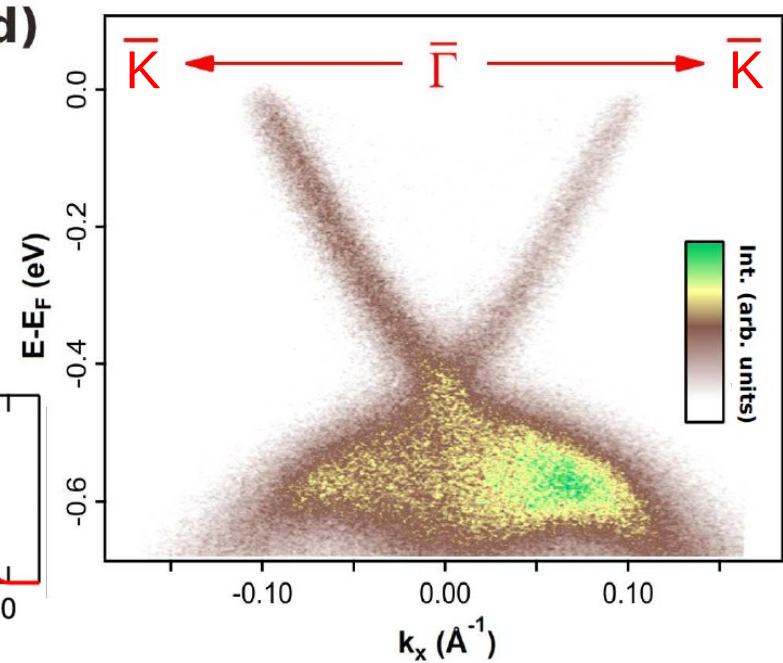
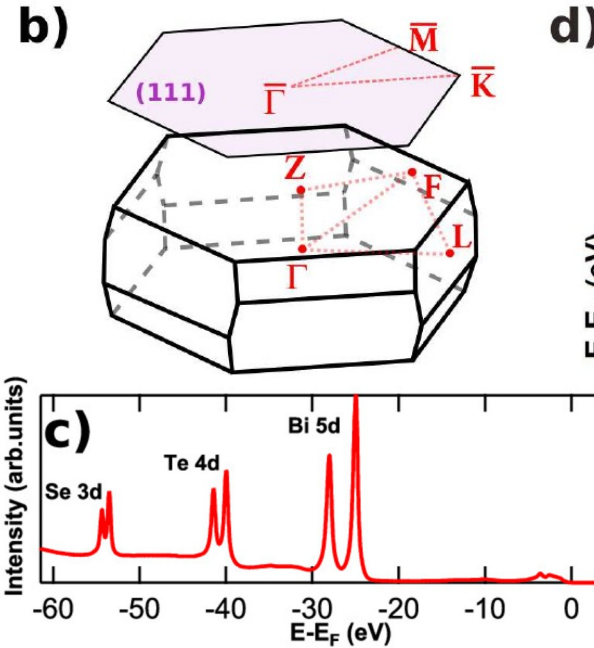
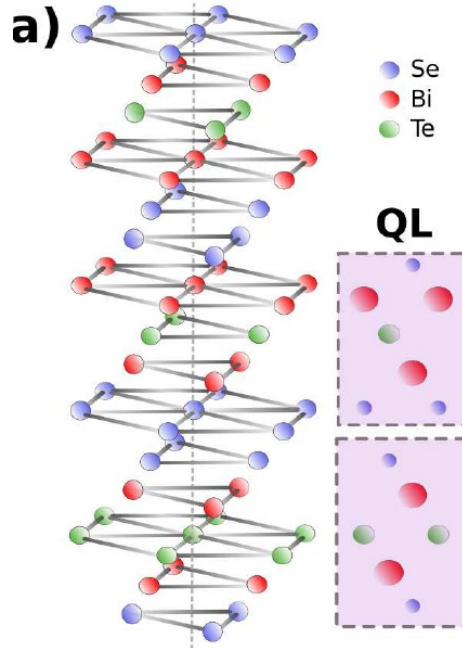
Se	Bi	Te
Bi	Se	Se
Se	Bi	Te
Bi	Se	Se



- 3D quintuple layer crystal structure.
- **Brillouin zone (BZ)** and projected **surface BZ** of Bi₂Se₂Te.



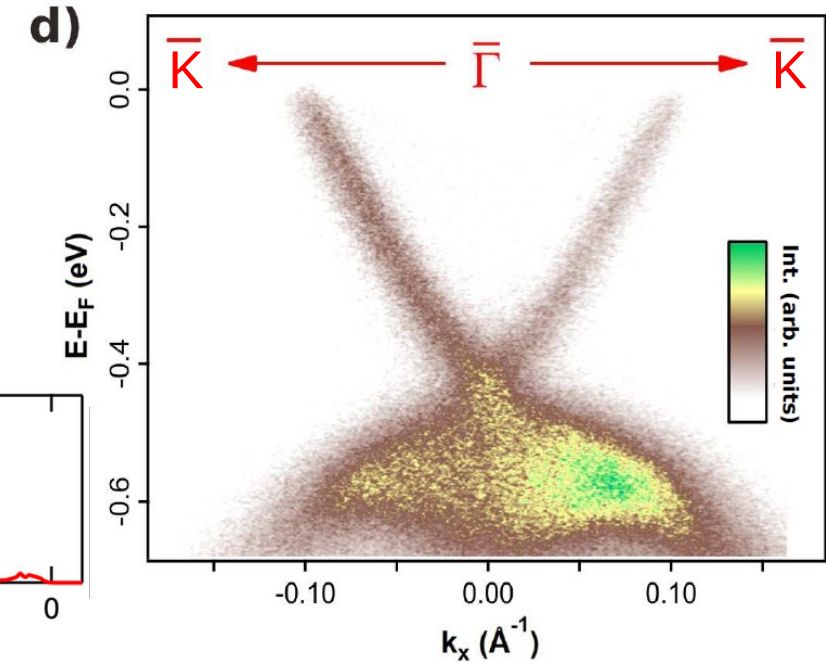
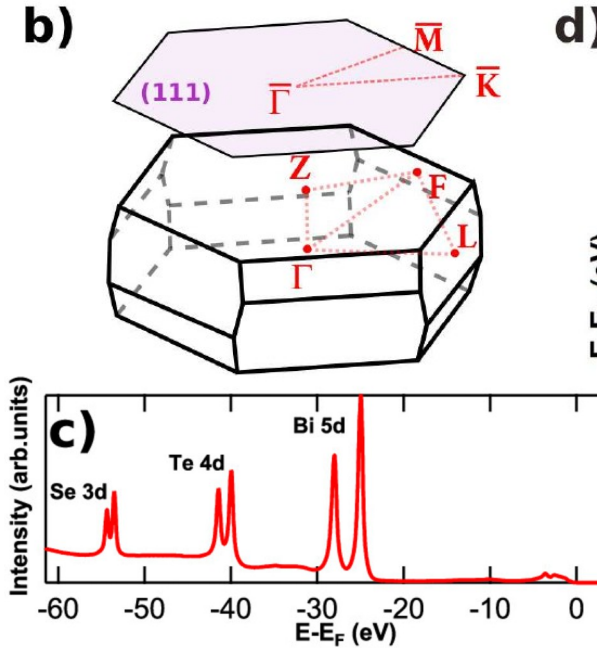
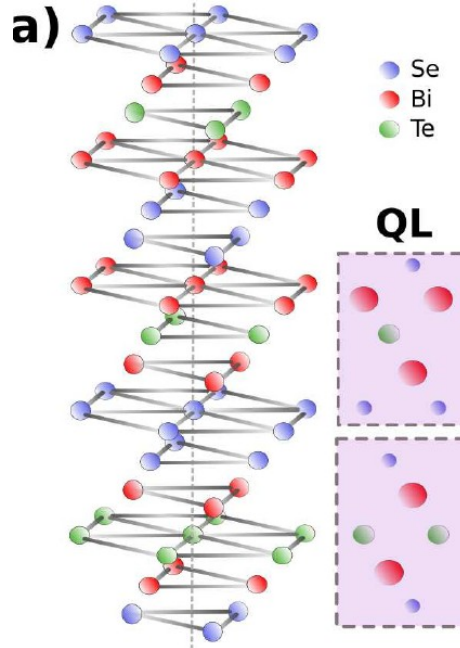
Results: pristine $\text{Bi}_2\text{Se}_2\text{Te}$



- 3D quintuple layer crystal structure.
- Brillouin zone (BZ) and projected surface BZ of $\text{Bi}_2\text{Se}_2\text{Te}$.
- **XPS** spectrum: **intense and narrow peaks**, very well defined **spin-orbit doublets** prove the **surface quality** after *in situ* exfoliation.



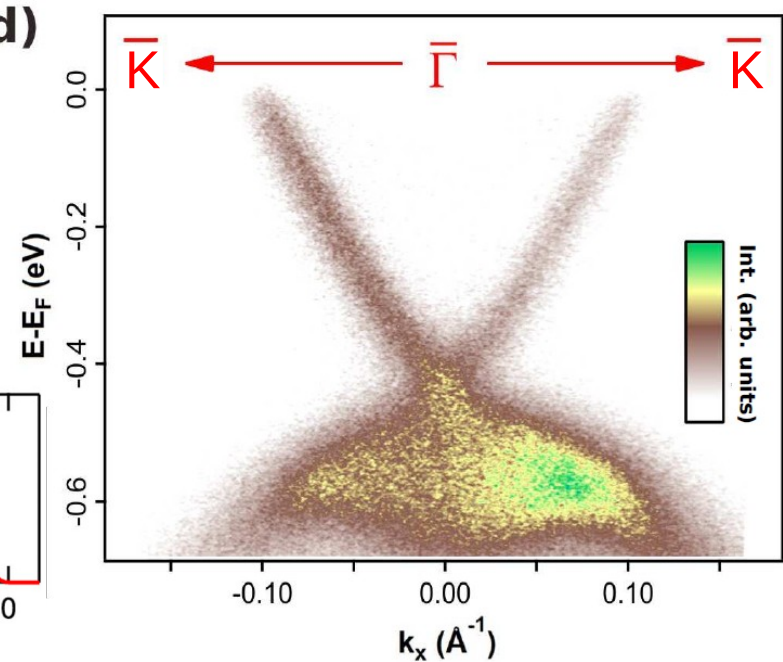
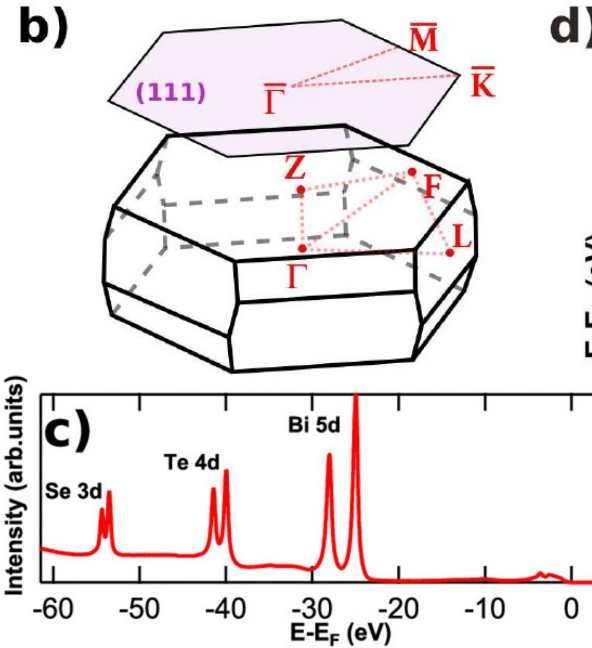
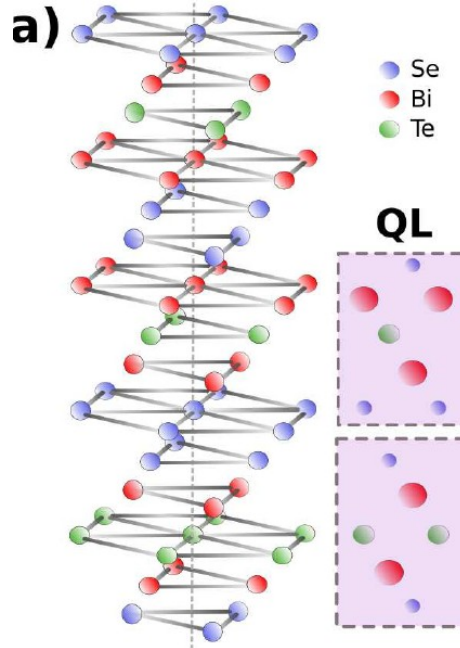
Results: pristine Bi₂Se₂Te



- 3D quintuple layer crystal structure.
- Brillouin zone (BZ) and projected surface BZ of Bi₂Se₂Te.
- XPS spectrum: intense and narrow peaks, very well defined spin-orbit doublets prove the surface quality after *in situ* exfoliation.
- Pristine Bi₂Se₂Te TSS ARPES bandmap along the Γ K direction yields:



Results: pristine Bi₂Se₂Te



- 3D quintuple layer crystal structure.
- Brillouin zone (BZ) and projected surface BZ of Bi₂Se₂Te.
- XPS spectrum: intense and narrow peaks, very well defined spin-orbit doublets prove the surface quality after *in situ* exfoliation.
- Pristine Bi₂Se₂Te TSS ARPES bandmap along the Γ K direction yields:

$$E_{DP} = 440 \text{ meV}$$

No gap

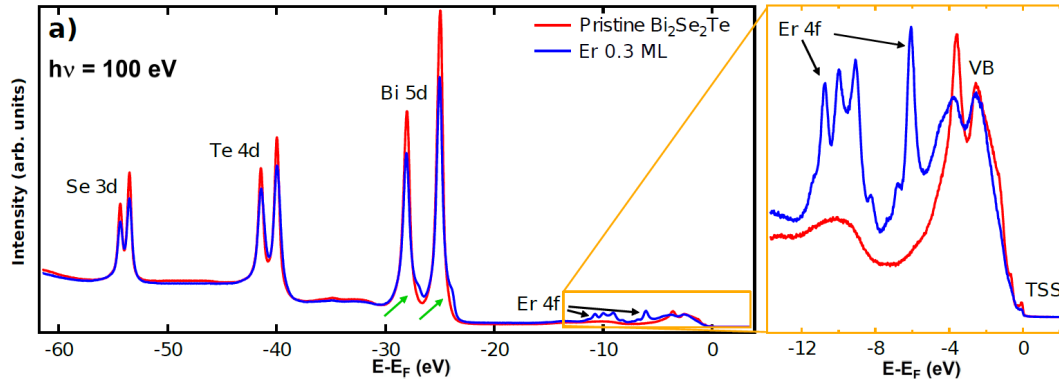
$$V_F = (7.1 \pm 0.1) \cdot 10^5 \text{ m/s}$$



Results: Er-doped $\text{Bi}_2\text{Se}_2\text{Te}$ XPS

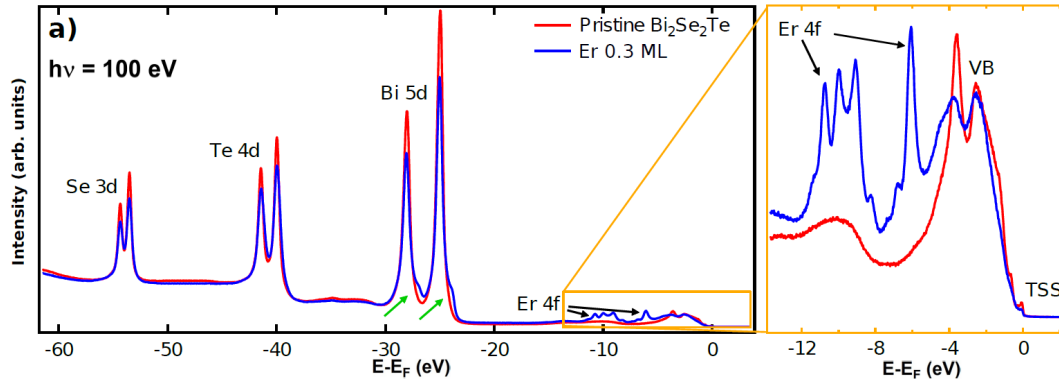


Results: Er-doped Bi₂Se₂Te XPS





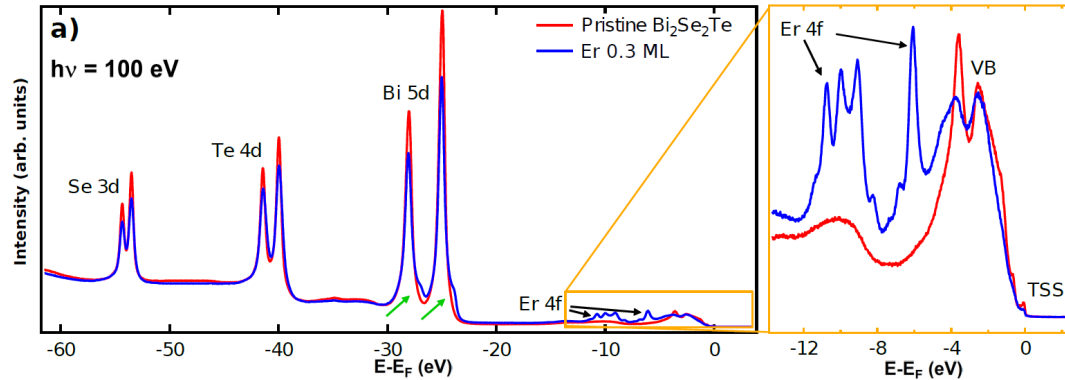
Results: Er-doped Bi₂Se₂Te XPS



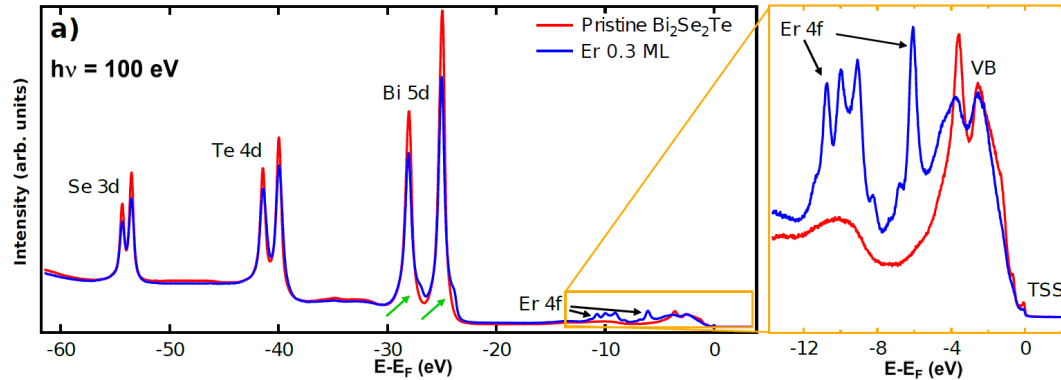
- Se 3d, Te 4d, Bi 5d → attenuated.



Results: Er-doped Bi₂Se₂Te XPS



- Se 3d, Te 4d, Bi 5d → attenuated.
- No extra components at higher BEs → **no surface oxidation or contamination**



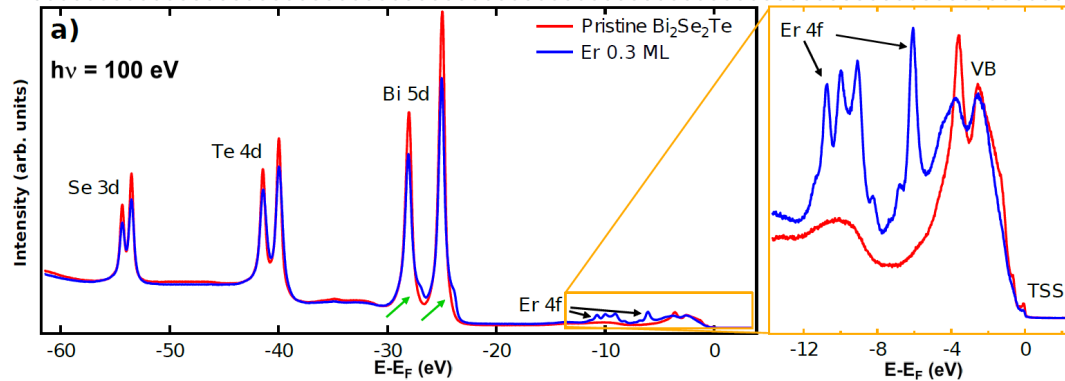
Results: Er-doped $\text{Bi}_2\text{Se}_2\text{Te}$ XPS

- Se 3d, Te 4d, Bi 5d → attenuated.
- No extra components at higher BEs → no surface oxidation or contamination
- No widening of the peak + very sharp and well resolved multipeak structure **Er 4f** states → **no further disorder introduced**





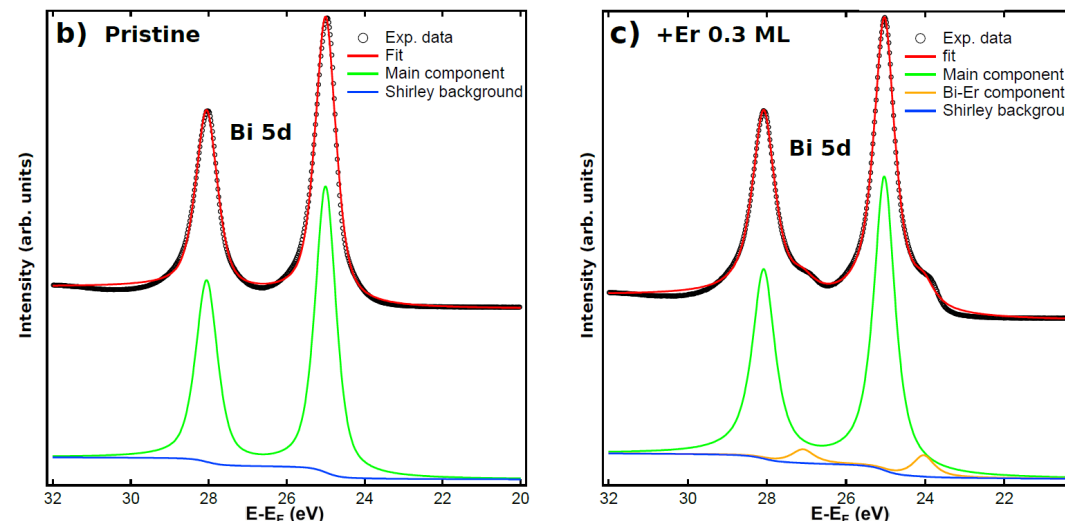
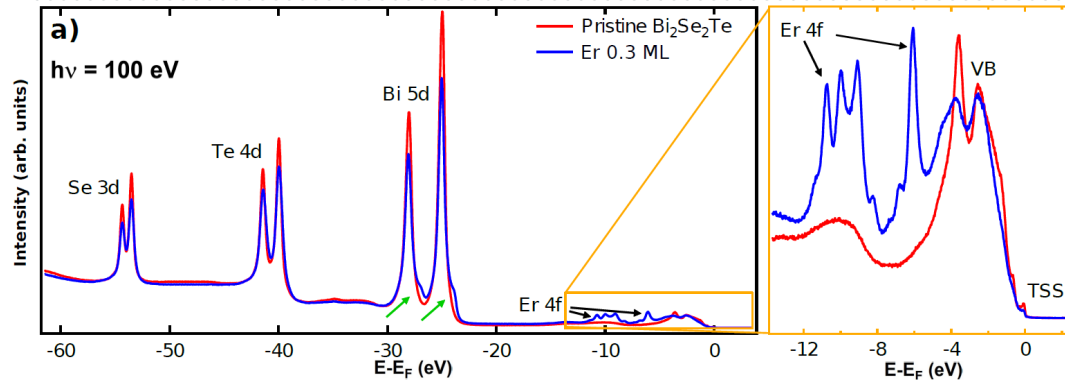
Results: Er-doped Bi₂Se₂Te XPS



- Se 3d, Te 4d, Bi 5d → attenuated.
- No extra components at higher BEs → no surface oxidation or contamination
- No widening of the peak + very sharp and well resolved multipeak structure **Er 4f** states → **no further disorder introduced**



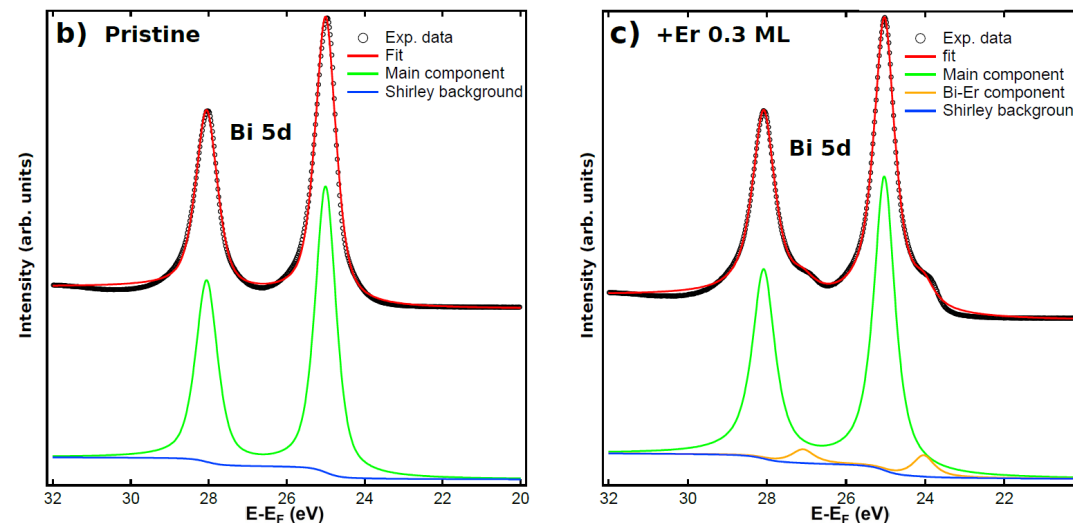
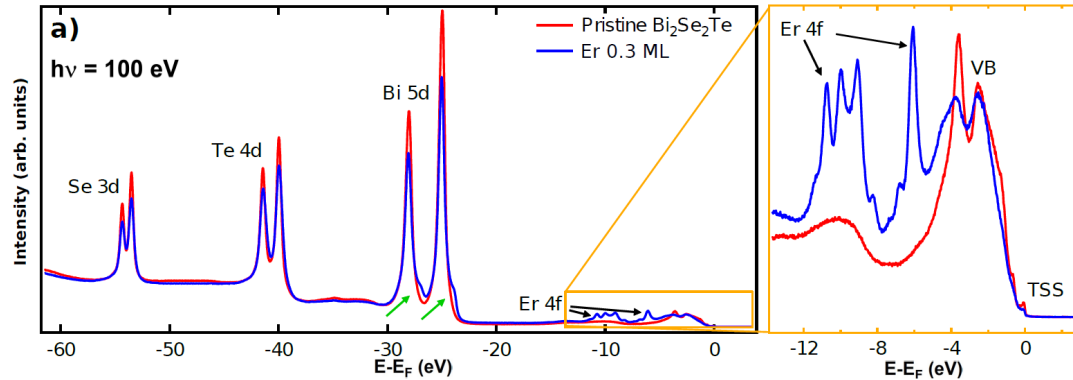
Results: Er-doped Bi₂Se₂Te XPS



- Se 3d, Te 4d, Bi 5d → attenuated.
- No extra components at higher BEs → no surface oxidation or contamination
- No widening of the peak + very sharp and well resolved multipeak structure Er 4f states → no further disorder introduced
- **Second Bi 5d component** → intensity linearly increases with the Er coverage → related to superficial **Bi-Er bond** + interaction at the RE-TI interface



Results: Er-doped Bi₂Se₂Te XPS



- Se 3d, Te 4d, Bi 5d → attenuated.
- No extra components at higher BEs → no surface oxidation or contamination
- No widening of the peak + very sharp and well resolved multipeak structure Er 4f states → no further disorder introduced
- Second Bi 5d component → intensity linearly increases with the Er coverage → related to superficial Bi-Er bond + interaction at the RE-TI interface
- Bi 5d peak attenuation → **Er coverage estimation**

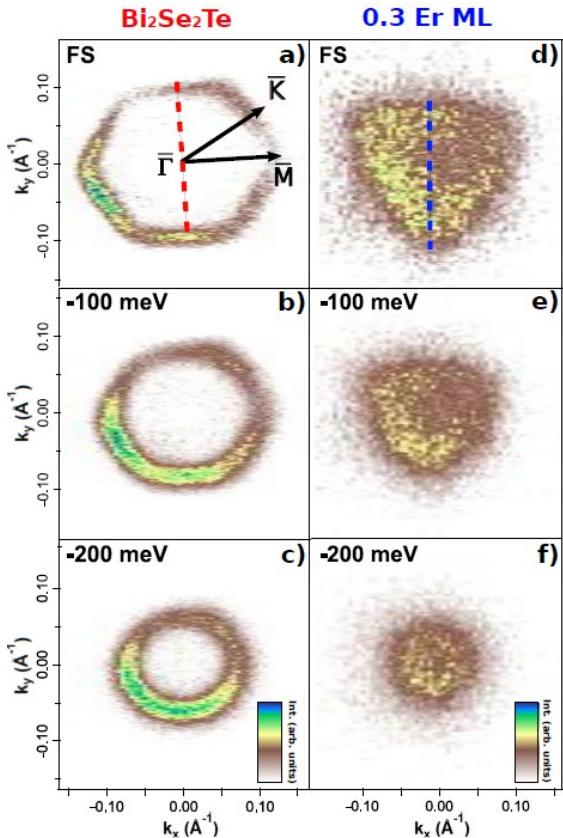


Results: pristine vs. Er-doped $\text{Bi}_2\text{Se}_2\text{Te}$ Fermi maps





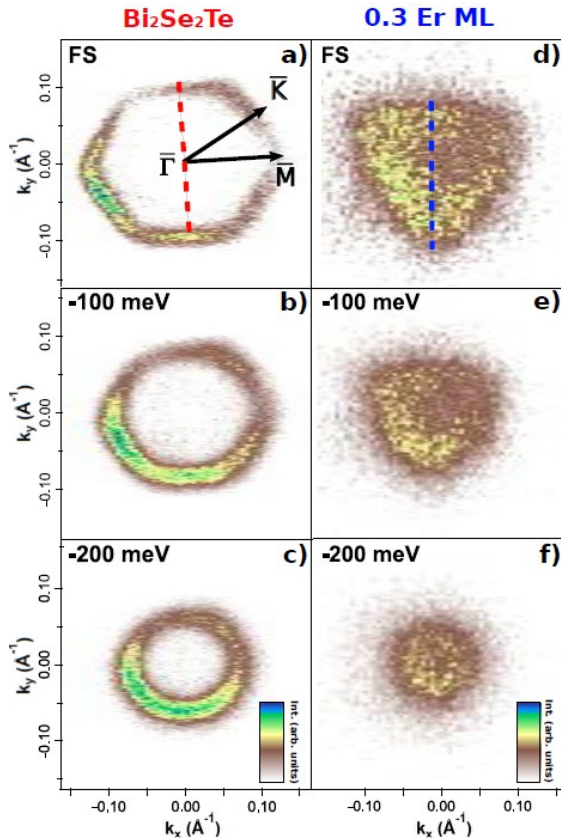
Results: pristine vs. Er-doped Bi₂Se₂Te Fermi maps



- Pristine BST TSS → hexagonal warped FS and the circular CE maps.



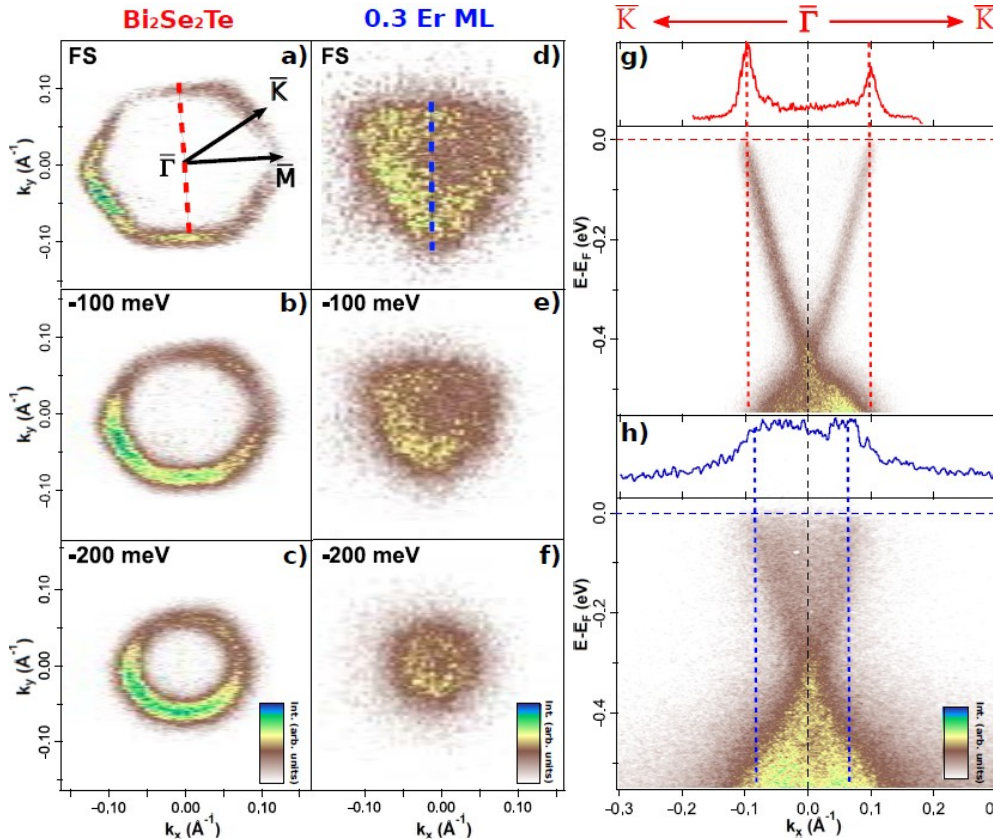
Results: pristine vs. Er-doped Bi₂Se₂Te Fermi maps



- Pristine BST TSS → hexagonal warped FS and the circular CE maps.
- **Er-doped** BST TSS → TSS warping symmetry: **hexagonal → trigonal**



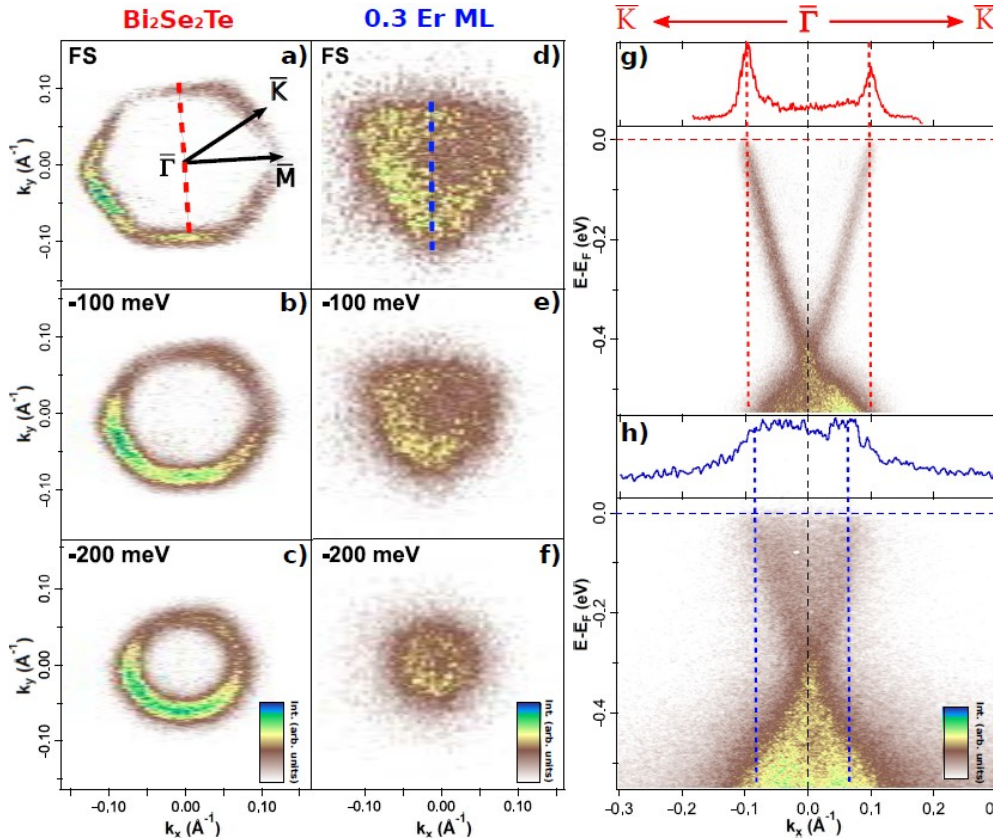
Results: pristine vs. Er-doped Bi₂Se₂Te Fermi maps



- Pristine BST TSS → hexagonal warped FS and the circular CE maps.
- Er-doped BST TSS → TSS warping symmetry: hexagonal → trigonal
- Induced inversion asymmetry in the TSS** band dispersion in along the Γ K direction



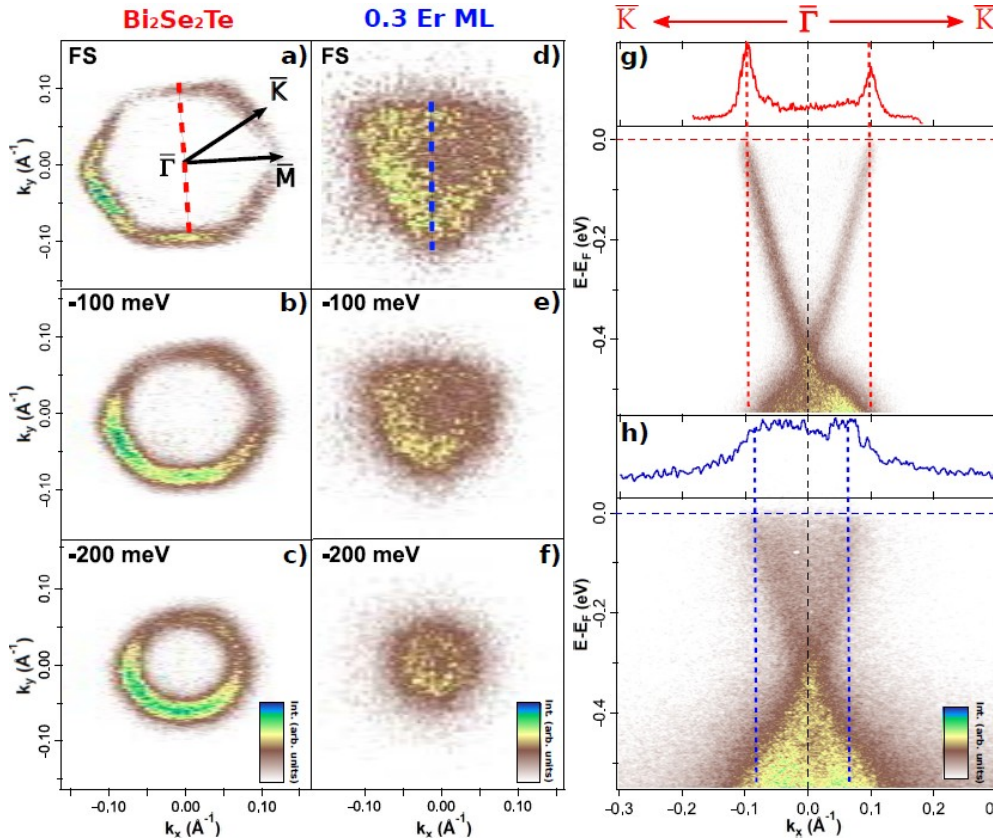
Results: pristine vs. Er-doped Bi₂Se₂Te Fermi maps



- Pristine BST TSS → hexagonal warped FS and the circular CE maps.
- Er-doped BST TSS → TSS warping symmetry: hexagonal → trigonal
- Induced inversion asymmetry in the TSS band dispersion in along the $\bar{\Gamma}\bar{K}$ direction
 - MDCs along dashed lines
 - Pristine** Bi₂Se₂Te: same branch v_F → **symmetric** k_F



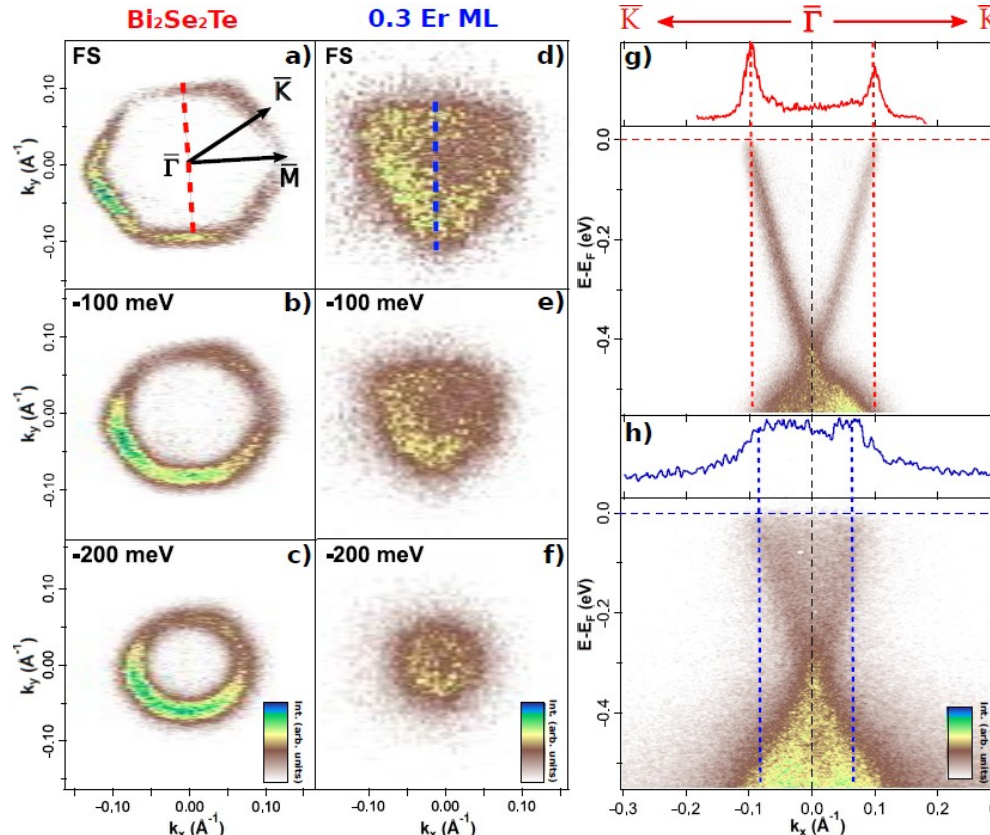
Results: pristine vs. Er-doped Bi₂Se₂Te Fermi maps



- Pristine BST TSS → hexagonal warped FS and the circular CE maps.
- Er-doped BST TSS → TSS warping symmetry: hexagonal → trigonal
- Induced inversion asymmetry in the TSS band dispersion in along the Γ K direction
 - MDCs along dashed lines
 - Pristine Bi₂Se₂Te: same branch v_F → symmetric k_F
 - Er-doped Bi₂Se₂Te:** different branch v_F → **asymmetric k_F**



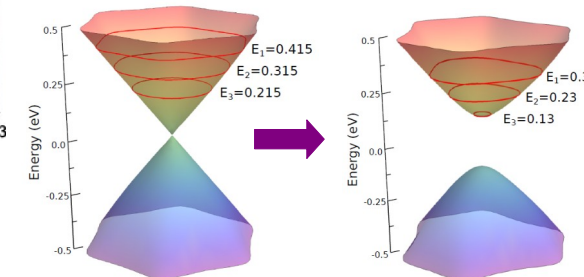
Results: pristine vs. Er-doped Bi₂Se₂Te Fermi maps



$$H = \hbar v_F (k_x \sigma_y - k_y \sigma_x) + (\lambda k^3 \cos 3\theta - \Delta) \sigma_z$$

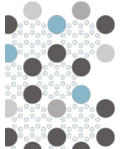
Muñiz Cano, B., et al. *Nano Lett.* **2023**, *23*, 13, 6249–6258

- Pristine BST TSS → hexagonal warped FS and the circular CE maps.
- Er-doped BST TSS → TSS warping symmetry: hexagonal → trigonal
- Induced inversion asymmetry in the TSS band dispersion in along the Γ K direction
 - MDCs along dashed lines
 - Pristine Bi₂Se₂Te: same branch v_F → symmetric k_F
 - Er-doped Bi₂Se₂Te: different branch v_F → asymmetric k_F
- Theoretical model → magnetic **Zeeman out-of-plane term in Hamiltonian**



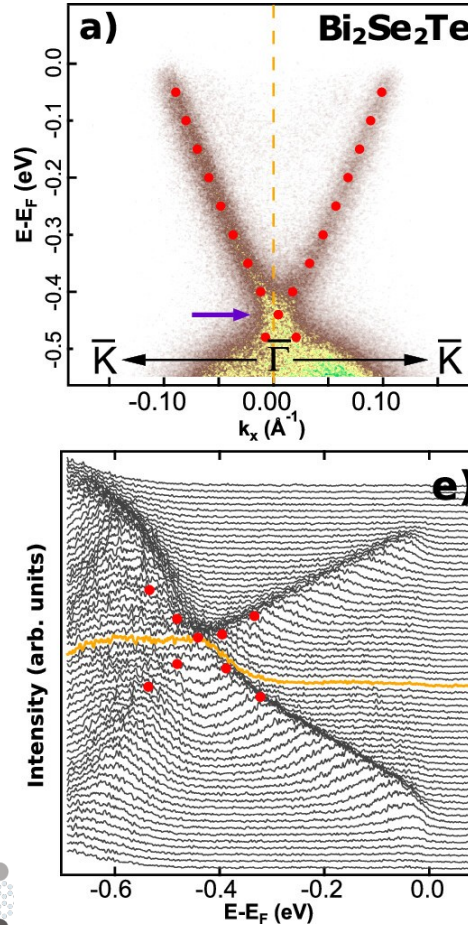


Results: bandgap opening at the Dirac point





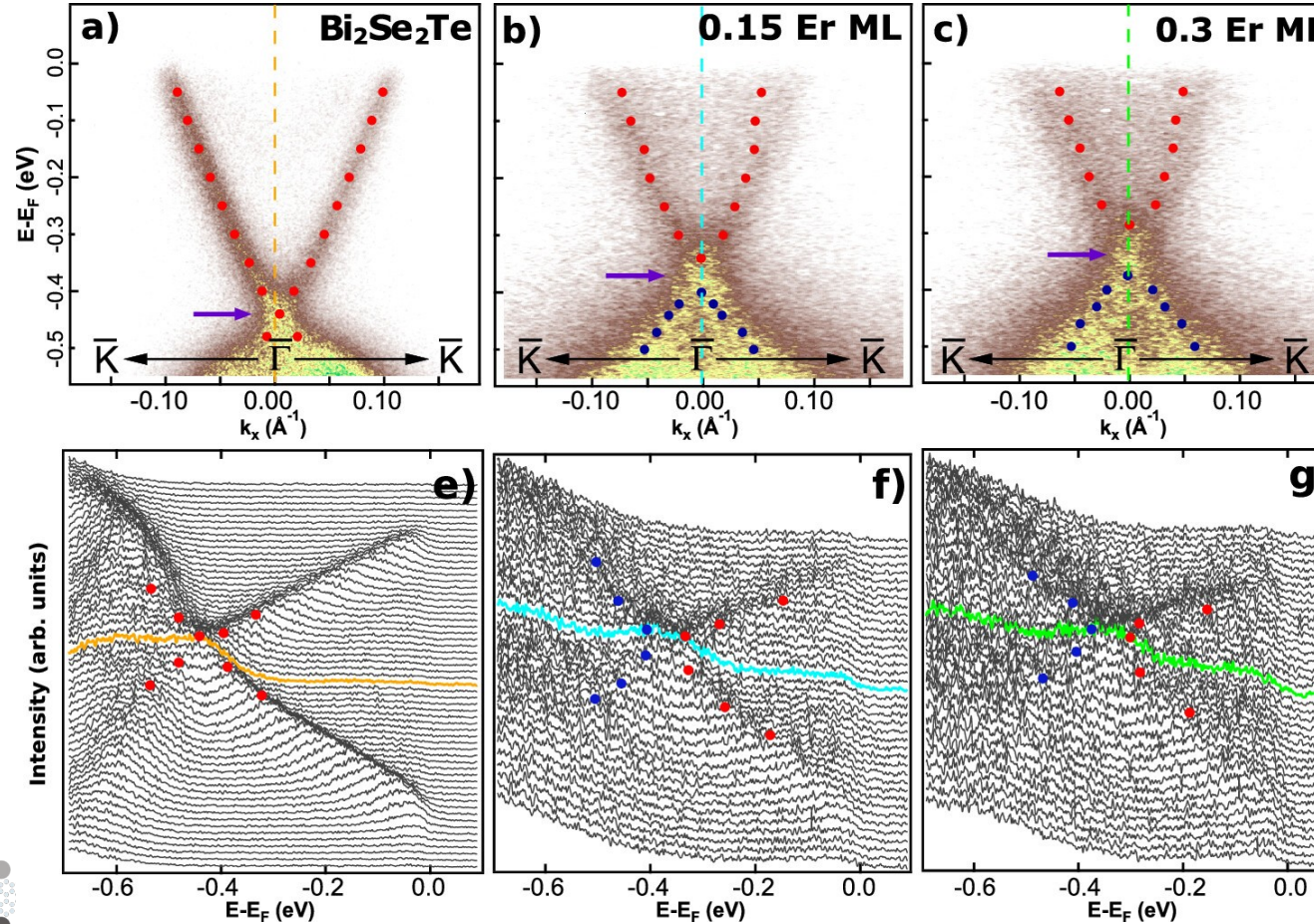
Results: bandgap opening at the Dirac point



- Pristine BST:
 - DP defined as intersection of two linear branches at 440 meV
 - Punctual maximum of intensity in the EDC at Γ



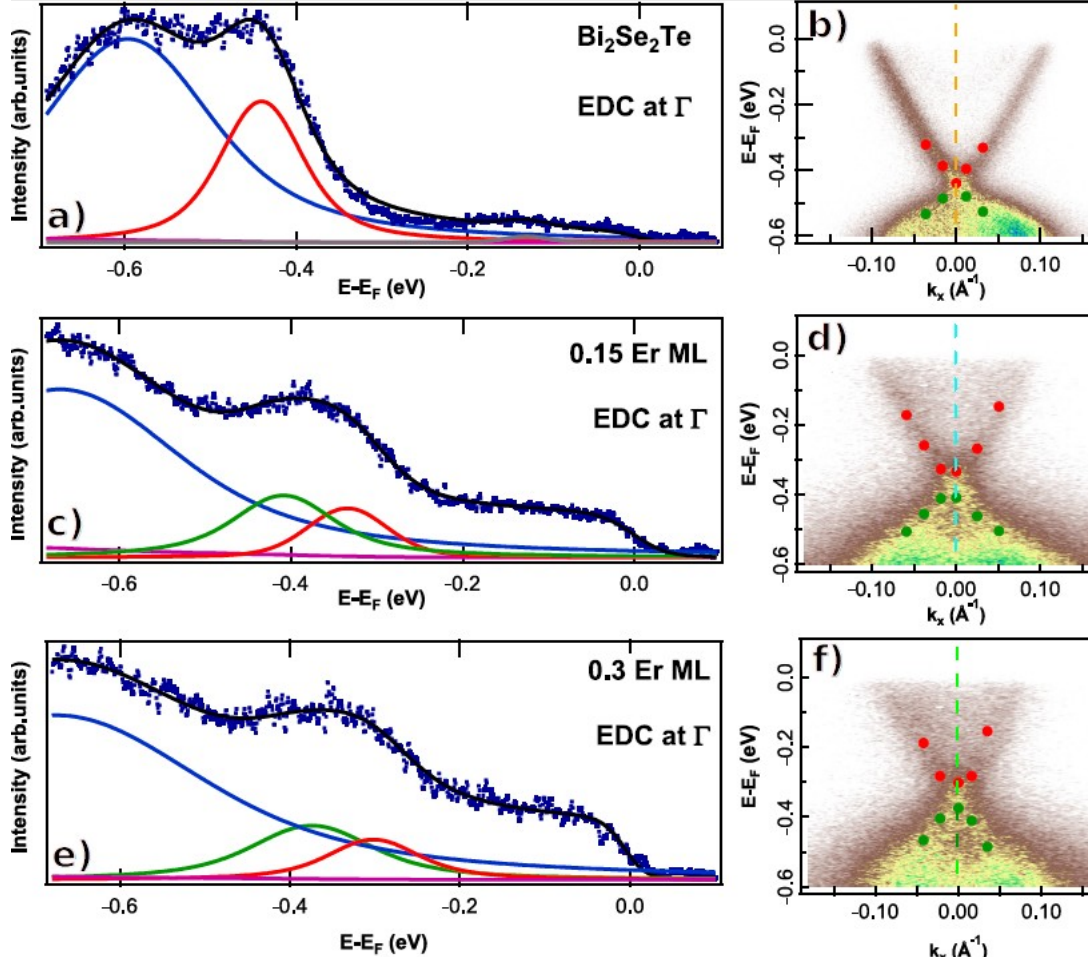
Results: bandgap opening at the Dirac point



- Pristine BST:
 - DP defined as intersection of two linear branches at 440 meV
 - Punctual maximum of intensity in the EDC at Γ
- Er-doped BST:
 - Linear dispersion renormalized to parabolic
 - Plateau in the EDC at Γ instead of maximum of intensity



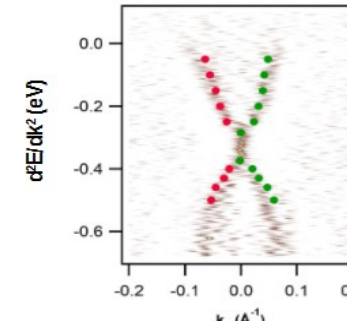
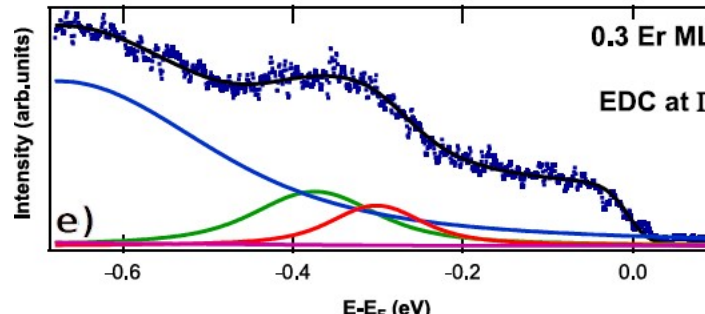
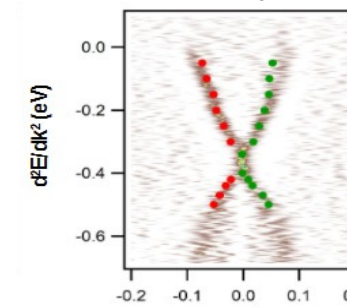
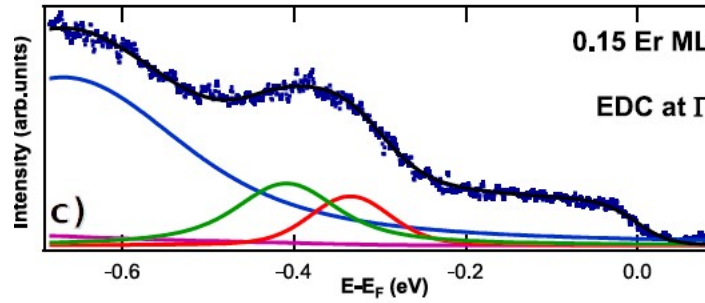
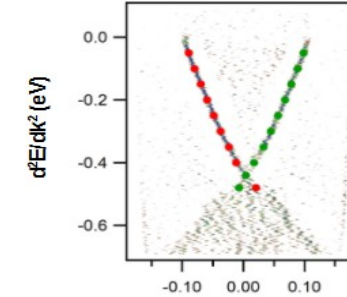
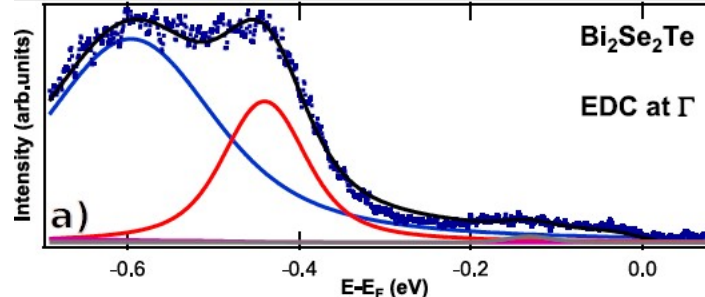
Results: bandgap opening at the Dirac point



- Pristine BST:**
 - **DP defined** as intersection of two linear branches at 440 meV
 - **Punctual maximum** of intensity in the EDC at Γ
- Er-doped BST:**
 - Linear dispersion renormalized to **parabolic**
 - **Plateau** in the EDC at Γ instead of maximum of intensity



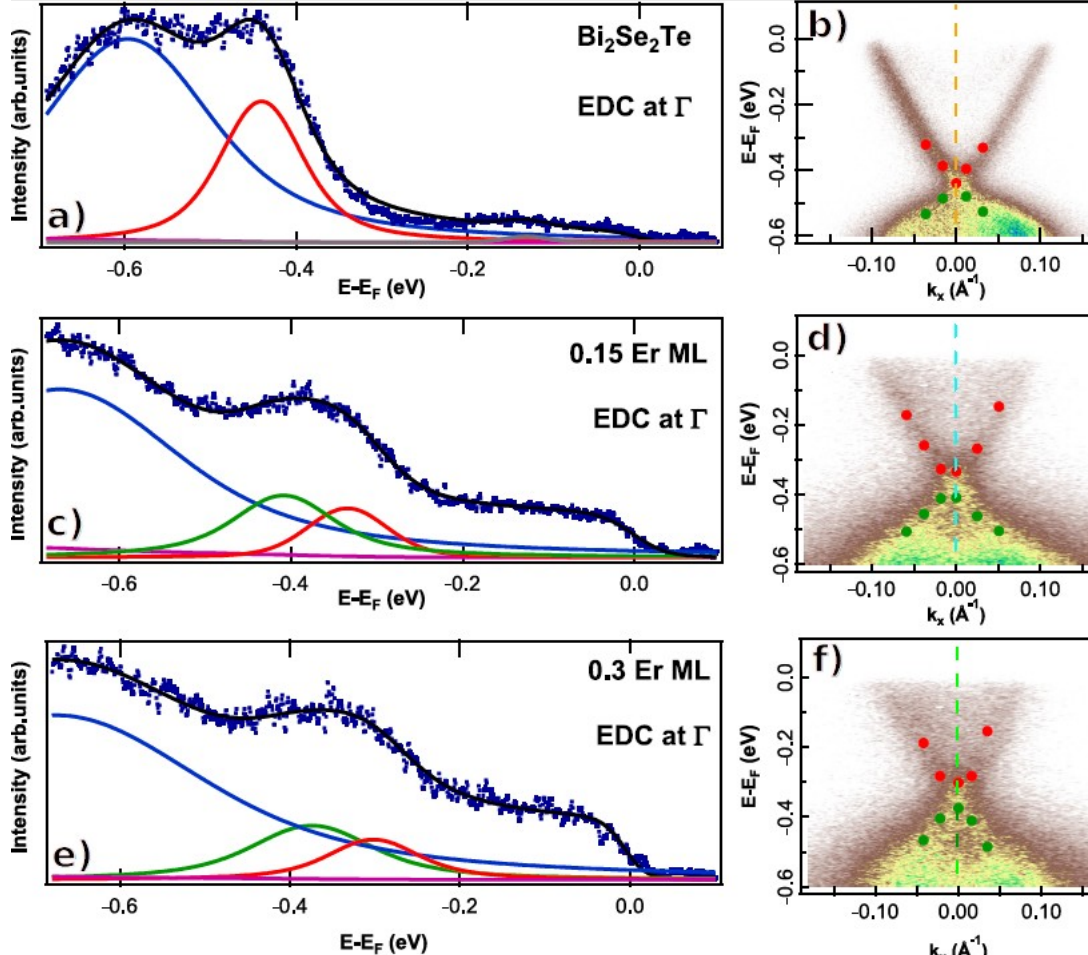
Results: bandgap opening at the Dirac point



- **Pristine BST:**
 - **DP defined** as intersection of two linear branches at 440 meV
 - **Punctual maximum** of intensity in the EDC at Γ
- **Er-doped BST:**
 - Linear dispersion renormalized to **parabolic**
 - **Plateau** in the EDC at Γ instead of maximum of intensity



Results: bandgap opening at the Dirac point



- **Pristine BST:**
 - DP defined as intersection of two linear branches at 440 meV
 - Punctual maximum of intensity in the EDC at Γ
 - **Er-doped BST:**
 - Linear dispersion renormalized to parabolic
 - Plateau in the EDC at Γ instead of maximum of intensity
- Gap opening**



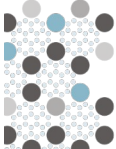
Summary and conclusions





Summary and conclusions

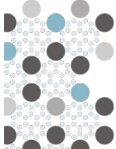
- Prototypical 3D TI Bi₂Se₂Te magnetically doped with low concentrations of Er





Summary and conclusions

- Prototypical 3D TI Bi₂Se₂Te magnetically doped with low concentrations of Er
- **Firts experimental observation** of the magnetically induced **transition** of the warping of the TSS from hexagonal to trigonal





Summary and conclusions

- Prototypical 3D TI $\text{Bi}_2\text{Se}_2\text{Te}$ magnetically doped with low concentrations of Er
- **Firts experimental observation** of the magnetically induced **transition** of the **warping** of the TSS from **hexagonal to trigonal**
- Signatures of the **bandgap opening**





Summary and conclusions

- Prototypical 3D TI $\text{Bi}_2\text{Se}_2\text{Te}$ magnetically doped with low concentrations of Er
- **Firts experimental observation** of the magnetically induced **transition** of the **warping** of the TSS from **hexagonal to trigonal**
- Signatures of the **bandgap opening**
- **p-type doping: tunability** of the **DP** towards the **Fermi level**





Summary and conclusions

- www.nanoscience.imdea.org
- Prototypical 3D TI $\text{Bi}_2\text{Se}_2\text{Te}$ magnetically doped with low concentrations of Er
 - **Firts experimental observation** of the magnetically induced **transition** of the **warping** of the TSS from **hexagonal to trigonal**
 - Signatures of the **bandgap opening**
 - **p-type doping: tunability** of the **DP** towards the **Fermi level**
 - Theoretical model with **Zeeman out-of-plane term** rationalizes the results and yields a large **exchange coupling** of **0.1 eV**





Summary and conclusions

- www.nanoscience.imedea.org
- Prototypical 3D TI Bi₂Se₂Te magnetically doped with low concentrations of Er
 - **Firts experimental observation** of the magnetically induced **transition** of the **warping** of the TSS from **hexagonal to trigonal**
 - Signatures of the **bandgap opening**
 - **p-type doping: tunability** of the **DP** towards the **Fermi level**
 - Theoretical model with **Zeeman out-of-plane term** rationalizes the results and yields a large **exchange coupling of 0.1 eV**
 - **Controlled doping of TIs with REs** as an excellent approach to realize the **QAHE at higher temperatures** since it fulfills all its requirements



Acknowledgements



Spin-ARPES Laboratory:
Beatriz Muñiz Cano
Miguel Ángel Valbuena
CONPHASE™

Rodolfo Miranda
Julio Camarero Francisco Guinea



EXCELENCIA
SEVERO
OCHOA
EXCELENCIA
MARÍA
DE MAEZTU

First-Principles Modelling for Quantum Materials
Yago Ferreiros
Pierre A. Pantaleón
Jose Angel Silva-Guillén



Physics and Engineering of Nanodevices (PEND)
Adriana I. Figueroa
Sergio O. Valenzuela
Atomic Manipulation and Spectroscopy (AMS)
Kevin García Díez
Aitor Mugarza



Horizon 2020
European Union funding
for Research & Innovation



European Union
European Regional Development Fund
Investing in your future

BL20 – LOREA
Ji Dai
Massimo Tallarida



Vera Marinova





Thank you!



